



Fermi National Accelerator Laboratory

FERMILAB-FN-623

Longitudinal Wakefield Focusing: An Unconventional Approach to Reduce the Bunch Length in Tevatron

A. Gerasimov

*Fermi National Accelerator Laboratory
P.O. Box 500, Batavia, Illinois 60510*

July 1994



Longitudinal wakefield focusing: an unconventional approach to reduce the bunch length in Tevatron.

A.Gerasimov

Fermi National Accelerator Laboratory,*
P.O.Box 500, Batavia, IL 60510, USA

August 11, 1994

Abstract

A method is discussed for creating a strong potential well distortion effect in proton storage rings that would allow the possibility for achieving shorter bunch lengths. The insertion device having the necessary capacitive impedance is the ferrite-lined waveguide with foreshortened ends. The cavity thus obtained is designed to have a single dominant mode with high enough quality factor so that the wakefield energy is transferred from bunch to bunch. In order to be compressed in a shorter length by a factor of two, long bunches $l \approx 30cm$, with number of particles per bunch $N_p = 10^{11}$, would require the length of the structures $L \approx 73m$. For shorter bunches, $l = 15cm$, one needs $L = 41m$ for $N_p = 5 \cdot 10^{10}$.

1 Introduction

Achieving shorter bunch length in the Tevatron would provide a better information on the primary vertex and would allow collider experiments to use shorter vertex detector [1]. A shorter bunch length would also allow an increase of luminosity by reducing the β -functions at the interaction point. The conventional approaches for achieving the goal of shorter bunches have

*Operated by the Universities Research Association, Inc. under contract with the U.S.Dept. of Energy.

been either through the use of higher RF voltages or through increasing the number of RF cavities. Both of these options come at prohibitive expense /2/. Herein an alternative solution of “wakefield focusing” is proposed which builds upon the ideas of Alexei Burov /3-5/ for electron storage rings.

The effect of bunch shortening in electron rings, as described by Burov /3,4/, is with regard to the longitudinal wakefield $W(s)$, which stays nearly constant up to the distances Δs much larger than the bunch length σ and results in the potential well distortion that causes a significant shortening of the bunch length for large enough wakes. It is assumed that the wakefields decay within one revolution period so that the corresponding impedance is broadband. The existence of the strong shortening of bunch length was demonstrated formally by constructing an approximate solution of the Haissinski equation for the bunch distribution at thermal equilibrium in a self-distorted potential well, in the limit of a strong distortion. That limit is defined by the condition of the large “distortion parameter” k :

$$k = \frac{N e^2 W_{max}}{\kappa l} \gg 1 \quad (1)$$

with the number of particles N , electron (proton) charge e , wakefield magnitude W_{max} at $s = 0$, bunch length l , and the RF rigidity κ .

The basic physics of the shortening phenomenon quite simply relates to the fact that particles at the rear of the bunch are affected by the wakefield produced by particles at the front of the bunch. Given a flat (step-function) wakefield the particles at the rear of bunch will be decelerated more strongly than those particles at the front of the bunch. Furthermore, for energies above transition, the longitudinal “mass” is negative, and the reduction in energy incurs the reduction in the revolution period. Subsequently, above transition the particles at rear of bunch will tend to “catch up” with those particles at the front of bunch, so that the wakefields will provide an extra focusing and the bunch length is reduced. Below the transition energy, the effect of the wakefield is opposite and the bunch length is increased. The magnitude of the wakefield-induced “attraction” force of the front and the rear parts of the bunch is proportional to the magnitude of the wakefield and independent of the bunch length. This feature is an inherent advantage of the wakefield focusing over the conventional RF focusing, where the potential well is quadratic and the focusing force is proportional to the bunch length.

In order to apply wakefield focusing to any hadron machine in general, the Tevatron in particular, two major issues need to be resolved. The first issue stems from the realization that no thermal mechanisms such as syn-

chrotron radiation and its quantum fluctuations are present in the hadron ring, so the Haissinski equation analysis for the bunch shortening in electron rings /3/ is not applicable. Instead, the evolution of the single-particle distribution function obeys the Vlasov equation of a Hamiltonian dynamics and the phase-space density conservation. Because of conservation, the best possible compression of the bunch is achieved through the adiabatic turn-on of the wakefields. As a result, the density of the bunch then becomes non-gaussian in both momentum and coordinates, while for the electron rings the distribution in momentum does not change. The characteristic strength of the bunch compression, $G = l_0/l > 1$ in the asymptotic limit $k \gg 1$ is estimated from phase-space conservation to be:

$$G \sim k^{1/3} \quad (2)$$

For electron rings, the momentum spread is maintained constant by the synchrotron radiation irrespective of the focusing. The scaling of the bunch compression that results is $G \sim k$ /3/, thus the payoff for an increased focusing is much less for the proton ring case. The difficulty is a familiar one from normal RF focusing, where the bunch length scales with RF voltage V as $\sigma \sim 1/\sqrt{V}$ for the electron rings and $\sigma \sim V^{-1/4}$ for proton rings.

The second major issue is that of creating the capacitive impedance of the required strength. An approximate capacitive structure, with a finite "step length" of the wakefield function $W(s)$, was proposed in Ref./5/ in the form of a dielectric channel. The length of the "step" s_{max} scales with the internal radius of the channel, a as $s_{max} \sim a/4$. To gain significant compression, the condition $s_{max} > 3\sigma_0$ (where σ_0 is the initial half-max width of the longitudinal distribution, $\sigma_0 = l_0/4$ for a Gaussian distribution) must also be satisfied /3,5/. Therefore, the necessary internal channel radius for the Tevatron, with bunch $\sigma_0 = 60cm$ must be quite large, namely $a \approx 7m$. The wakefield for that radius would be far too weak for effective focusing.

An alternative source of the capacitive impedance is the gap of a "deep cavity" (see Ref./6/). Numerical simulations of the wakefields induced by a gap(s) +cavity system indicates that the discharge of the gap capacitance(s) on the outer surface of the pipe does not allow the wakefield to be made large enough without losing the step-like character of the wake. An improvement is proposed in the form of a ferrite-lined waveguide. This is similar to the idea of a dielectric channel, but with two essential modifications: a) enclosing the ferrite (dielectric) inside the pipe and making it into a cavity (see below) recycles the energy of the Cherenkov radiation (wakefields), and b) using the

ferrite instead of the dielectric substantially $\sim \sqrt{\mu}$ increases the wavelength of the wakefield.

The results of the numerical simulation of beam dynamics in the presence of a broadband capacitive impedance are presented. The adiabatic compression is indeed achieved, and its maximum value is defined by the condition that the total energy dissipation in the broadband impedance does not exceed the maximum available accelerating power of the RF cavity. For the parameters of the Tevatron, for which the bunch length /RF wavelength ratio is approximately 0.2, the maximum possible compression turns out to be quite small $\Delta\sigma/\sigma_0 \sim 25\%$ (note the low power in the scaling formula (2)!).

A significant modification of the wakefield focusing idea is proposed in this paper which removes the fundamental energy balance limitation inherent in previous methods and leads, as a result, to the possibility for a much stronger focusing. These improvements over previous method are accomplished with the use of a *narrowband* impedance waveguide rather than a dielectric channel which has a broadband impedance response. The wakefield energy is returned then back to the beam rather than being dissipated.

2 Structures with capacitive impedance.

2.1 Gaps.

A simple structure that is known to produce a capacitive impedance is the flat-flanked gap in a round pipe of the vacuum chamber, which is a part of a “deep” cavity /6/. An example is shown in Fig.1a, in which the axial symmetry is implied, r is the radial coordinate, and the beam is passing along the axis z . On the other side of the gap, a large chamber is placed. All walls are assumed to be made of a low-resistivity metal and the geometry is one of the standard designs of RF cavities /7/.

Qualitatively, creating the capacitive impedance by a gap is as follows: when the image charge, carried by the beam on the internal side of the pipe, reaches the gap, it is left behind the beam on one flank of the gap. At the same time, the anti-image charge is recreated on the other flank to compensate for the new image charge that continues along the pipe with the beam. The gap then will be left charged as a normal capacitor, with the charge exactly equal to that of the beam.

The qualitative description based on the image charge is confirmed by the graphs of Fig.1a-c, in which electric field patterns simulated with the

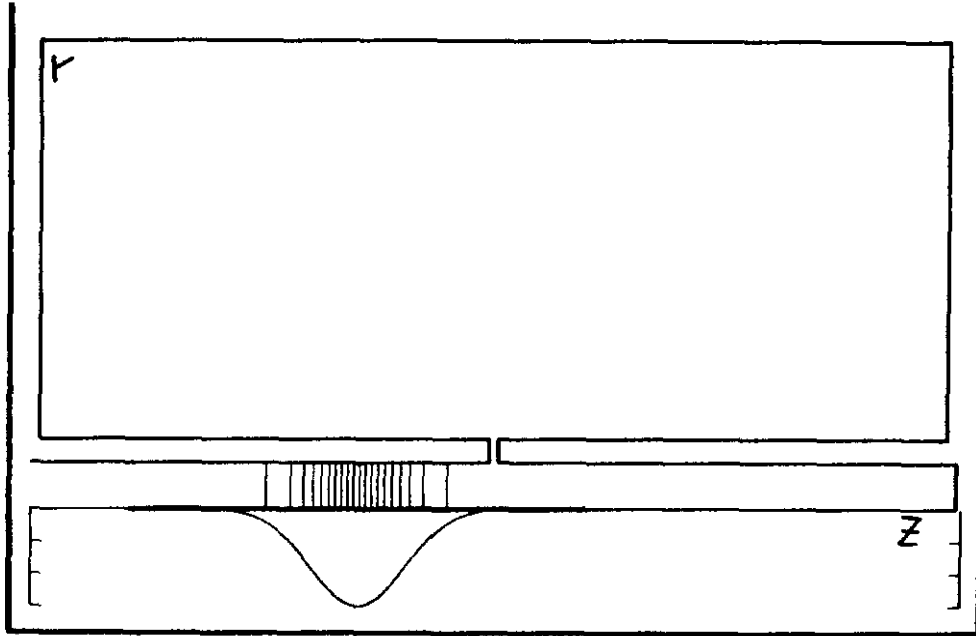


Fig.1a-j Electric field lines evolution for the gap-cavity system with parameters $r = 5.$, $\Delta = 2.5$, $h = 1.$, $R = 50.$, $L = 100.$ (all in *cm*). Bunch profile is shown under the axis. Bunch sigma is $\sigma = 5.$ (*cm*).

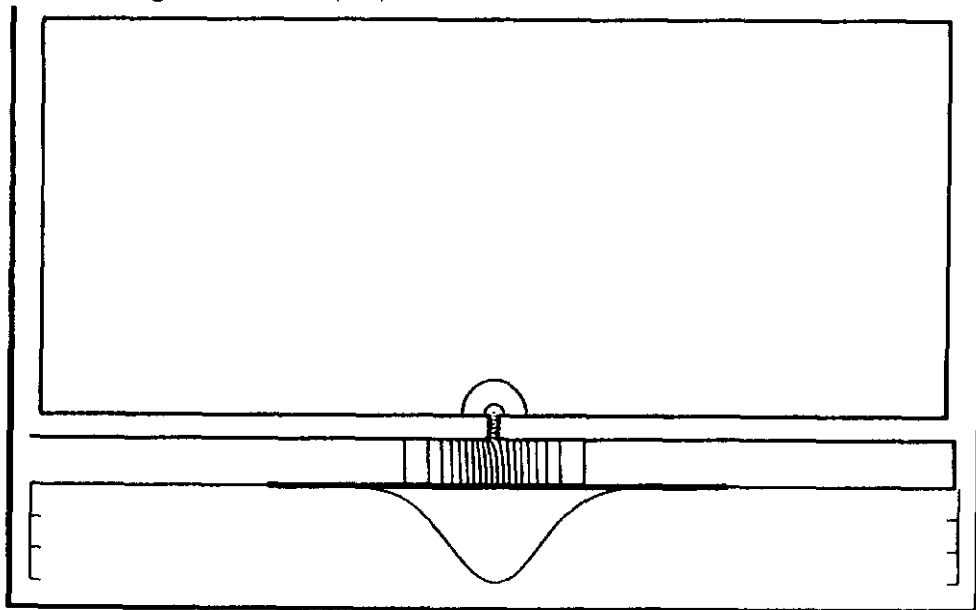


Fig.1b

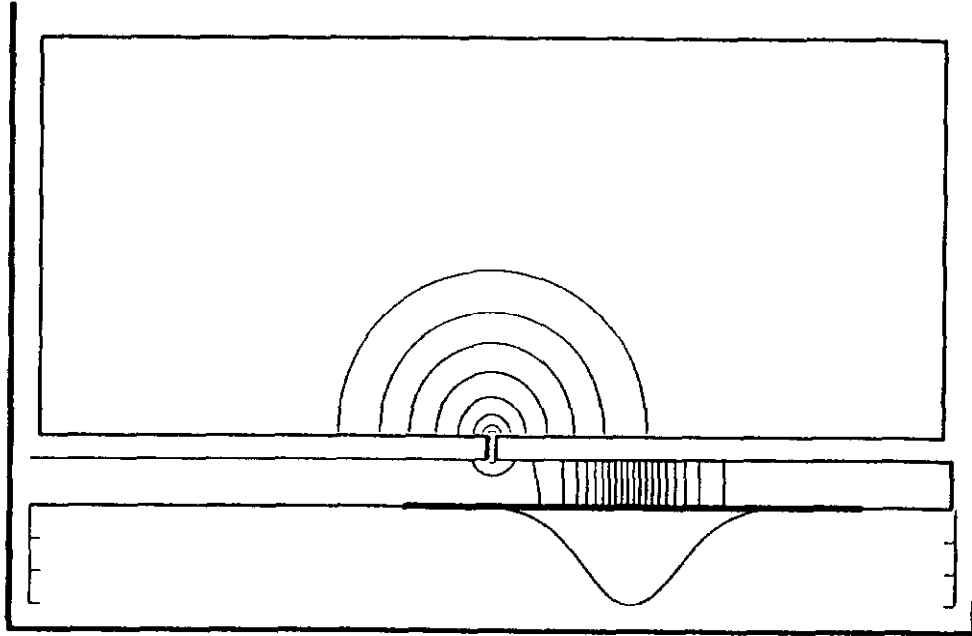


Fig.1c

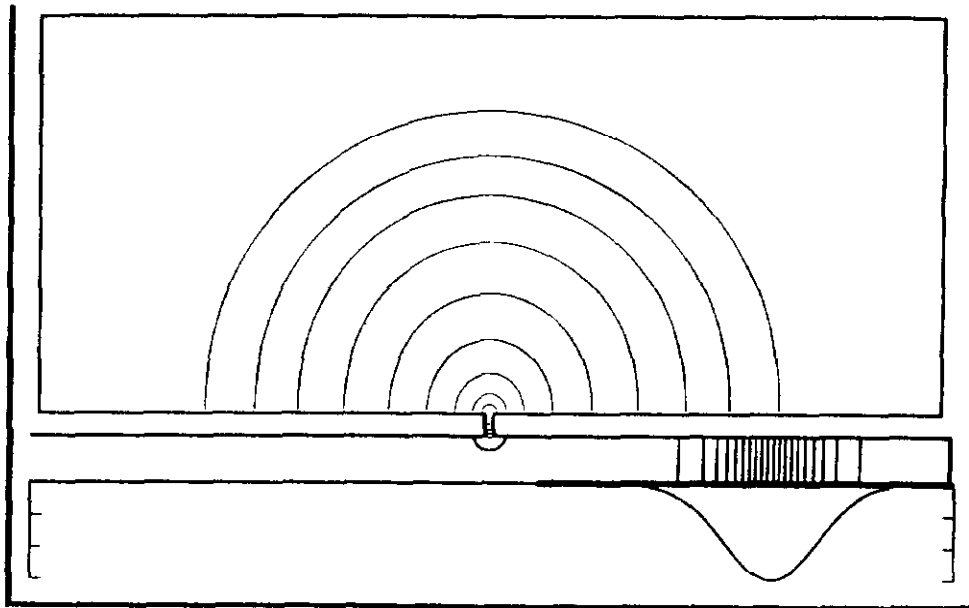


Fig.1d

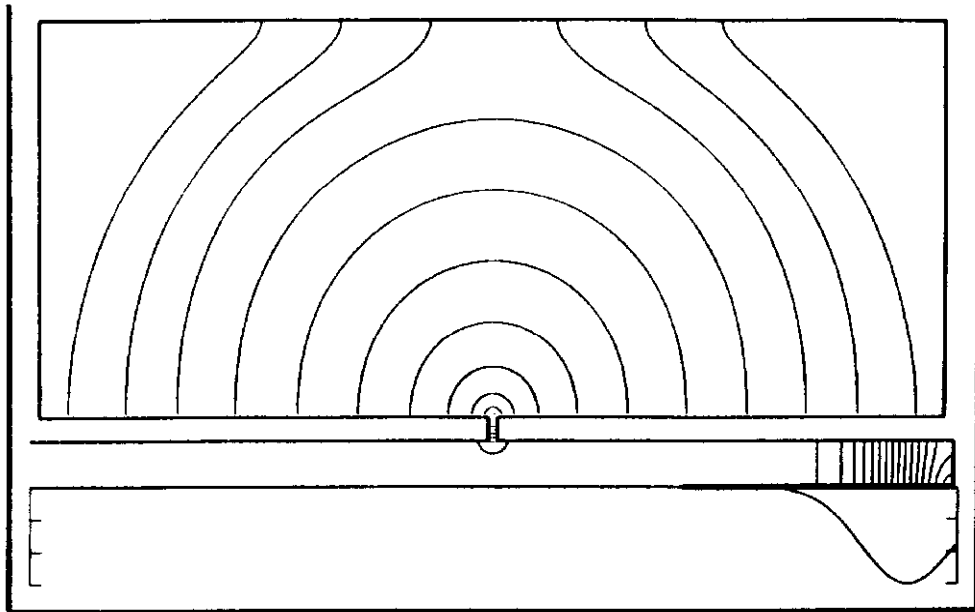


Fig.1e

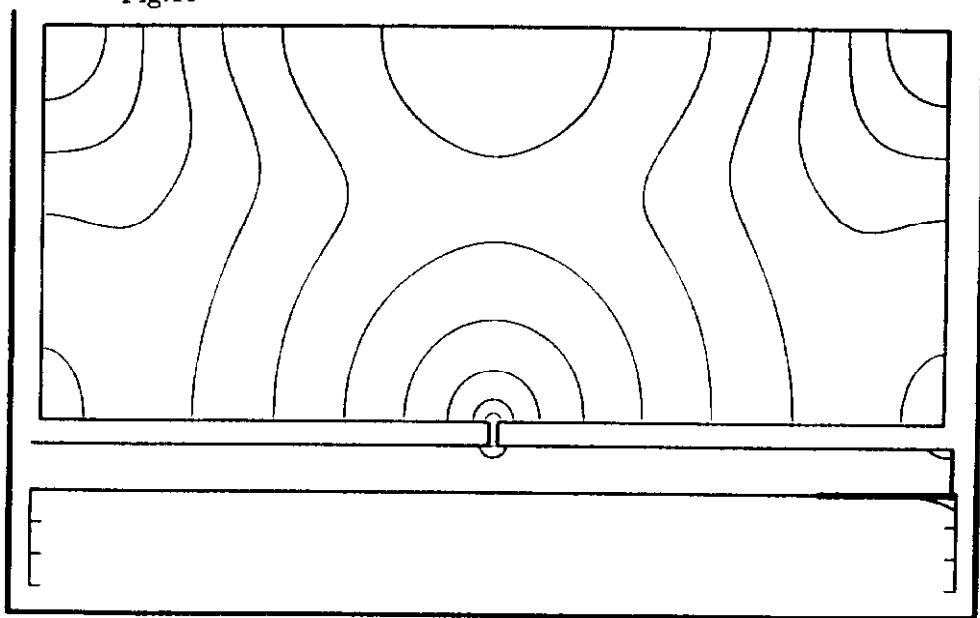


Fig.1f

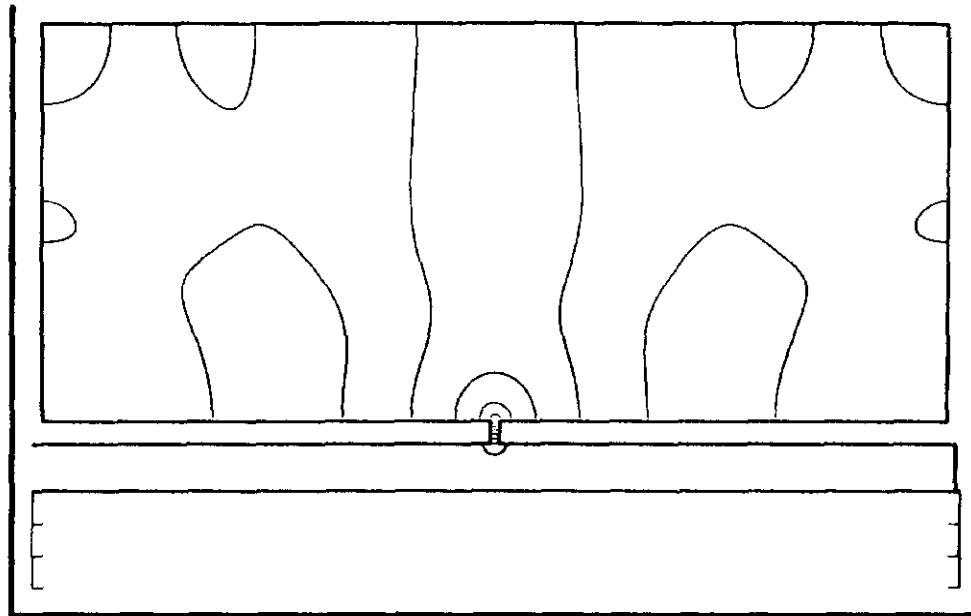


Fig.1g

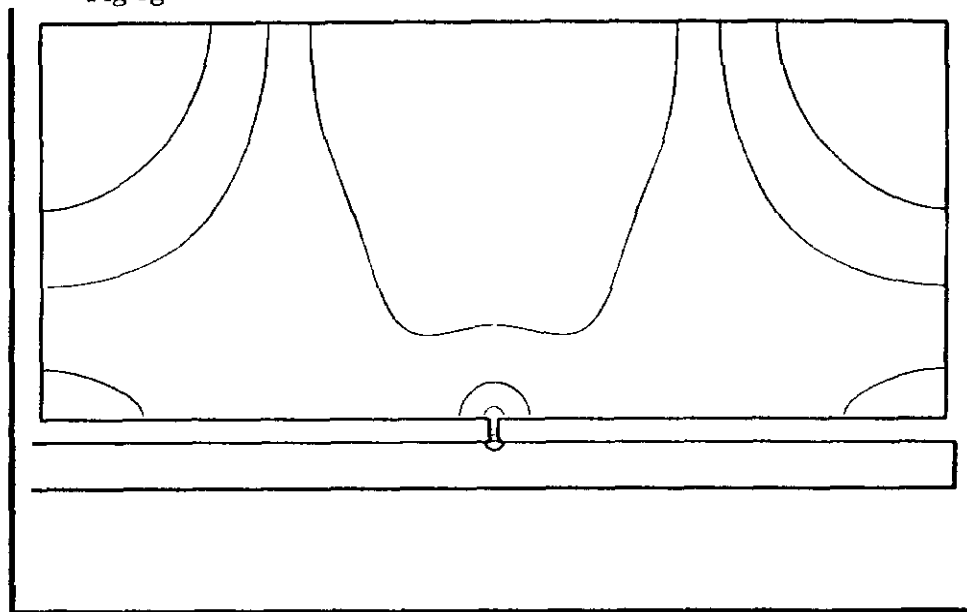


Fig.1h

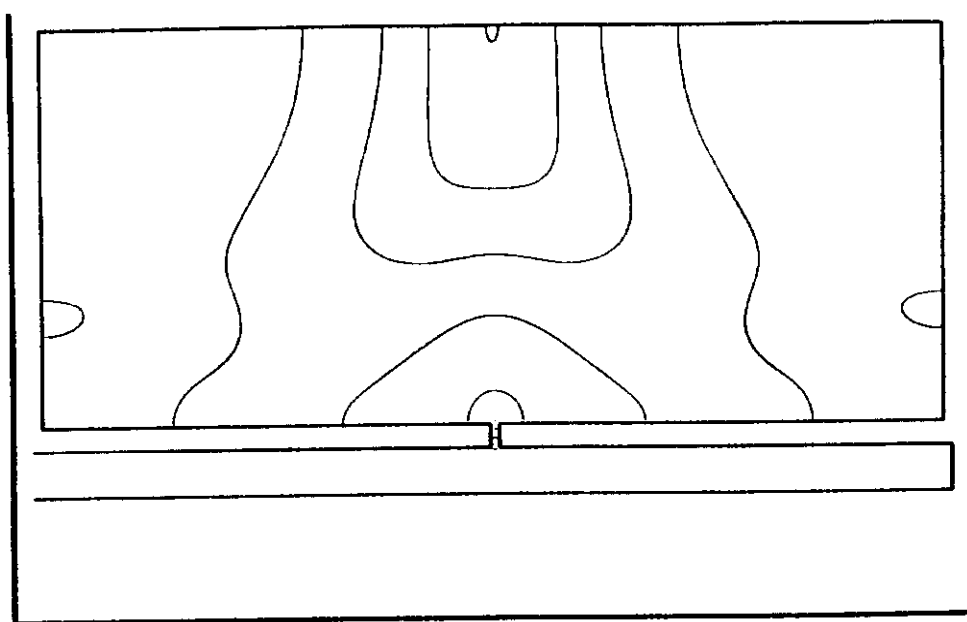


Fig.1i

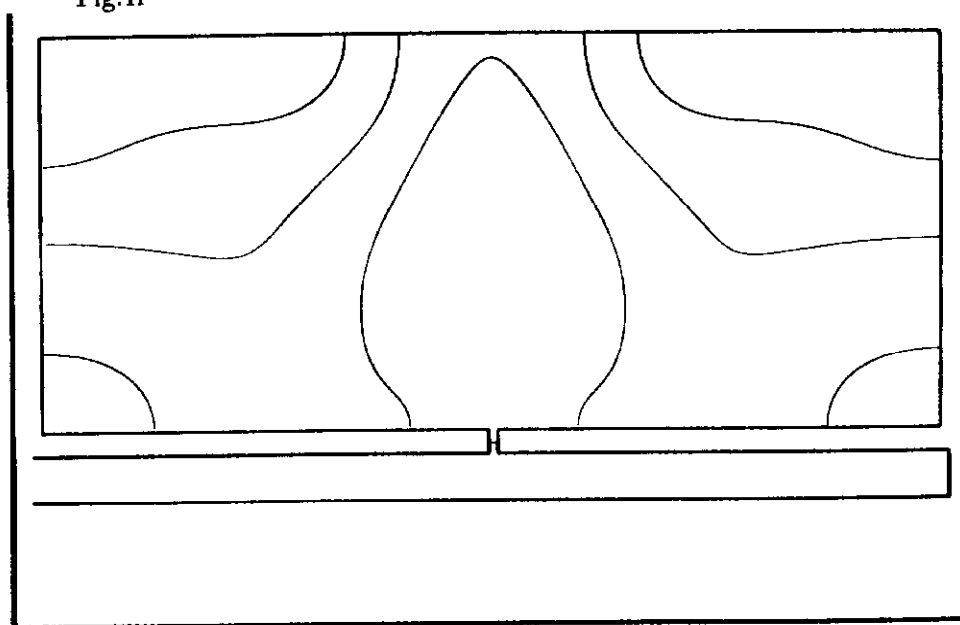


Fig.1j

use of the wakefield-calculation code TBCI /8/ are presented. The TBCI

code only allows the simulation of closed cavities, so a large cavity on the outside of the gap was added. The cavity-gap system is characterized by the internal pipe radius r , thickness of the wall Δ , gap length h , (external) radius of the cavity R , and cavity length L .

The useful effect of focusing in the broadband scheme comes from the gap itself, but the presence of the cavity walls does not affect the fields in the gap while the light travels to the wall and back. In Figs.1d-j the further evolution of the fields inside the structure is presented. The charge can be seen to be partially leaking from the gap to the outside walls with a time constant that depends on the geometry of the system. Simultaneously, the electromagnetic (RF) waves are excited inside the chamber with periodic pattern of oscillations. When the waves are reflected from the outside walls and return back at the gap, the field inside the gap is strongly disrupted. Thus, in order to keep the gap charged at nearly the initial voltage for a longer time, the outside chamber is chosen to be rather large. The wakefield function $W(s)$, obtained using the same computer code through a numerical integration of the electrical field at the location of the particle trailing behind the beam near the inner wall of the pipe /8/, is presented in Fig.2.

The scale of the wakefield is such that the maximum negative value of $W(s)$ in this graph is $W_{max} = -5 \cdot 10^{10}$ (V) for the charge of the bunch $Q_b = 1$ (Coulomb) and the horizontal scale of the graph is in meters. The σ of the probing bunch was chosen to be quite short; $\sigma = 5cm$, since the quantity of interest is the "point charge wakefield". After reaching a maximum at distances $\sim 2\sigma$ behind the peak of the bunch density, the wake function decreases and starts oscillating almost periodically (which should be interpreted as that mostly the fundamental mode of the cavity is excited). The discharge time constant and the period of oscillations are two distinct parameters that depend on the geometry of the gap-cavity system. For the purpose of focusing with broadband impedances, the wakefield has to stay nearly constant after reaching its maximum for a few sigmas of the bunch distribution (see /3,4/ and Section 3). In the new scheme of focusing with narrowband-type of wake that is proposed in Section 3.2, there is no need to have the wakefield not to change sign for more than σ . For the bunches in the Tevatron with $\sigma \approx 15cm$, this condition is satisfied, though the wakefield

decreases after reaching the maximum.

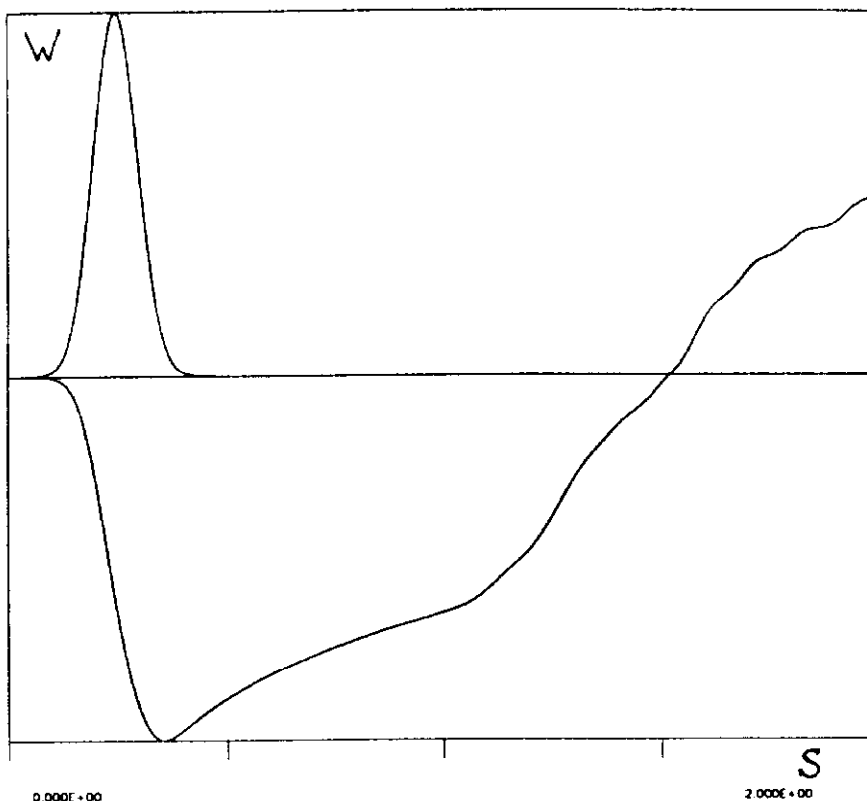


Fig.2 Wakefield function $W(s)$ for the case of Fig.1.

In order to have the maximum possible wakefield focusing in the broadband scheme, one needs to achieve the total wakefield potential W_{max} which equals the maximum RF potential V_{RF} (see /3,4/ and Section 3). For the Tevatron, for which $V_{RF} \sim 1MV$ and bunch intensities are about $N_p \sim 1.2 \cdot 10^{11}$ (particles per bunch), one can estimate the necessary gap capacitance $C = \frac{\epsilon_0 \Delta}{h}$ (with r for the inner pipe radius, Δ the thickness of the wall, and h the gap length) as $C \approx .14 \cdot 10^{-3}$ (m). It was assumed here that the gap satisfies the "flat capacitor" restrictions $h \ll \Delta$ as well as the condition $\Delta \ll r$. The small capacitance creates two problems. First, a substantial reduction in Δ or equivalently an increase in h from the values of the example in Fig.2 with $C = .125$ (m) can not be made without violating the "flat capacitor" restriction. The restriction of the flat capacitor is necessary to avoid fringe fields which increase the capacitance. The difficulty can

be circumvented however by using many identical gaps in a row, with thin conducting layers between them. The effective length h of the row is the sum of lengths of the individual gaps. The second difficulty is much more fundamental and comes from the fact that the small gap capacitance means a short discharge time, which imposes a limitation on the useful wakefield voltage that can be generated per unit length.

2.2 Ferrite-lined waveguides.

A possible way of increasing the discharge time constant of the gaps that were described in the previous section is to fill the outer cavity (see Fig.1) with a ferrite possessing a high permeability, μ , that increases the inductance of the equivalent circuit and slows down the discharge. A further extension of the idea described above is the ferrite lined waveguide structure having a layer of ferrite on the interior wall. The ferrite lined waveguide is similar to the dielectric channel proposed by Burov /5/. The important difference from Burov's approach, however, is twofold: a) enclosing the ferrite (dielectric) inside the pipe and making it into a cavity (see below) recycles the energy of the Cherenkov radiation (wakefields), and b) using the ferrite instead of the dielectric substantially $\sim \sqrt{\mu}$ increases the wavelength of the wakefield. The longer wavelength is necessary yet difficult to meet condition for the proton bunches that are generally much longer than the electron ones. Recycling the energy of the wakefield removes the major limitation of the achievable bunch compression that is imposed by the requirement of power loss compensation (see Section 3).

The general theory of wakefields in a dielectric-lined waveguide was developed in Ref./9/ in connection with the wakefield acceleration schemes. Also included in reference /9/ is the case of a non-dispersive ferrite (frequency-independent μ, ϵ). For the lining with constant $\mu > 1$ and $\epsilon > 1$ there are always only a finite number of waveguide modes that propagate with the phase velocity that equals the velocity of the charge, which is close to the speed of light in vacuum, and only these modes are excited by the charge. The longitudinal "monopole" wakefield $W(s)$ is given by the sum over the contributions from each mode /9/:

$$W(s) = -\frac{4}{\epsilon a^2} \sum_{\lambda} F_{\lambda} \cos \left(\frac{x_{\lambda} s}{a \sqrt{\epsilon \mu - 1}} \right) \quad (3)$$

where a is the outer radius of the ferrite, and the eigenvalues x_{λ} are defined implicitly as the roots of a complex expression. Two extreme cases; a thin

lining $\epsilon(1 - b/a) \ll 1$ and a thick one $\epsilon(1 - b/a) \gg 1$ (b is the inner radius of the ferrite lining, which is same as the pipe radius) can be solved analytically. In the thin lining case, there is only one mode:

$$\begin{aligned} x_1 &= \sqrt{\frac{2\epsilon}{1 - b/a}} \\ F_1 &= 4. \end{aligned} \quad (4)$$

In the thick lining case, there are many modes present and the eigenvalues x_λ and amplitudes F_λ , for indices λ not too high can be expressed as:

$$\begin{aligned} x_\lambda &= \bar{x}_\lambda \\ F_\lambda &= \frac{2\pi x_\lambda Y_0(x_\lambda)}{\epsilon J_1(x_\lambda)} \end{aligned} \quad (5)$$

where \bar{x}_λ are the zeroes of the Bessel function $J_0(x)$, and $Y_0(x)$, $J_1(x)$ are respectively the Neumann function of order zero and Bessel function of the order 1. The expansion above is, however, not converging and is useful only for the analysis of the lower modes. A convenient manner for performing the summation is suggested in Ref./5/. It was noticed that the maximum eigenvalues in the summation are of the order of $bx_\lambda/2\epsilon a \sim 1$. Using the asymptotic expressions for the eigenvalues and substituting the summation by integration, the result for the wakefield is given by:

$$W(s) = \frac{4}{b^2} \exp\left(-\frac{2\epsilon}{b} \frac{s}{\sqrt{\mu\epsilon - 1}}\right) - \frac{0.37}{2\epsilon b^2} \quad (6)$$

Two conditions, $s < b\sqrt{\epsilon\mu - 1}$ and $s < (a - b)\sqrt{\epsilon\mu - 1}$, have to be satisfied in order for the formula (6) to be applicable. At larger s , $W(s)$ is defined by the antiperiodicity condition $W(s + (a - b)\sqrt{\epsilon\mu - 1}) = -W(s)$.

In order to understand the wakefields that are induced by a realistic ferrite, it is important to take into account the frequency dispersion $\mu(\omega)$. Indeed, assuming the parameters $\mu = 600$, $\epsilon = 10$, the maximum frequency of the thick-lining case is estimated, from $f_{max} = c\sqrt{\epsilon}/b\sqrt{\mu}$, to be $f_{max} \approx 150$ MHz even for a large inner radius $b = 10$ cm. That value of f_{max} is significantly higher than the roll-off frequency of any ferrite with $\mu = 600$, as can be seen from Fig.3a, where the initial permeability is plotted as a function of frequency for a typical family of high-frequency ceramic ferrites.

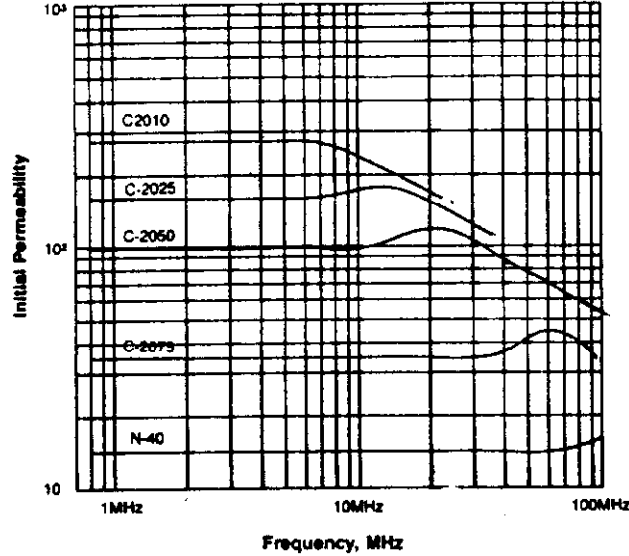


Fig.3a Frequency dependence of the real part of the magnetic permeability μ' for a typical family of high-frequency ferrites.

In Fig.3b, the dependence of the quality factor on the frequency is shown for the same family of ferrites as given in previous figure. One can see the losses increase significantly above the roll-off frequency.

The approach of the Ref./9/ may be extended to account for frequency dispersion, since the summation over modes emerges as pole contributions when performing the inverse Fourier transform from frequency domain back to time domain. Since the permeability μ is a complex quantity, the high-frequency poles lie off the real frequency axis. The result is the change of the amplitudes F_λ in formula (3) and the self-consistent selection of (complex) frequencies:

$$W(s) = -\frac{4}{\epsilon a^2} \sum_{\lambda} \text{Re} \left(\frac{F_{\lambda}}{1 + \frac{\omega_{\lambda}}{2\mu} \frac{d\mu}{d\omega}} \exp \left(i \frac{x_{\lambda} s}{a \sqrt{\epsilon \mu - 1}} \right) \right) \quad (7)$$

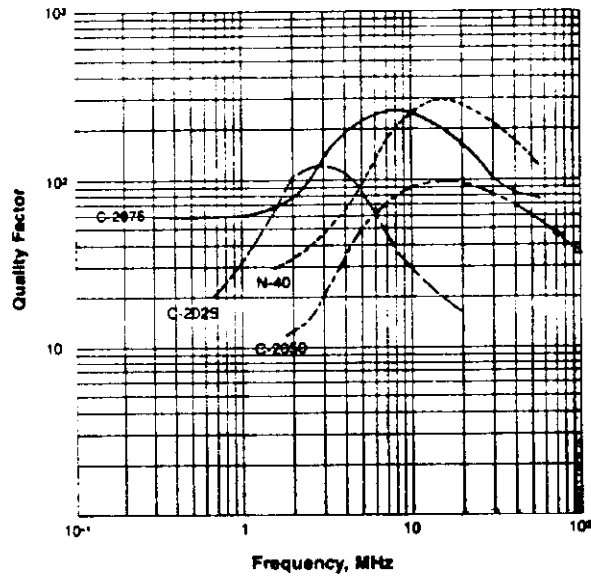


Fig.3b Quality factor as a function of frequency for the ferrites of Fig.3a.

Here, $\mu = \mu(\omega_\lambda)$, while the complex frequencies ω_λ are defined by solutions of the dispersion relation:

$$\omega_\lambda = \frac{x_\lambda c}{a\sqrt{\epsilon\mu(\omega_\lambda) - 1}} \quad (8)$$

which fall in the upper half-plane $Im(\omega_\lambda) > 0$.

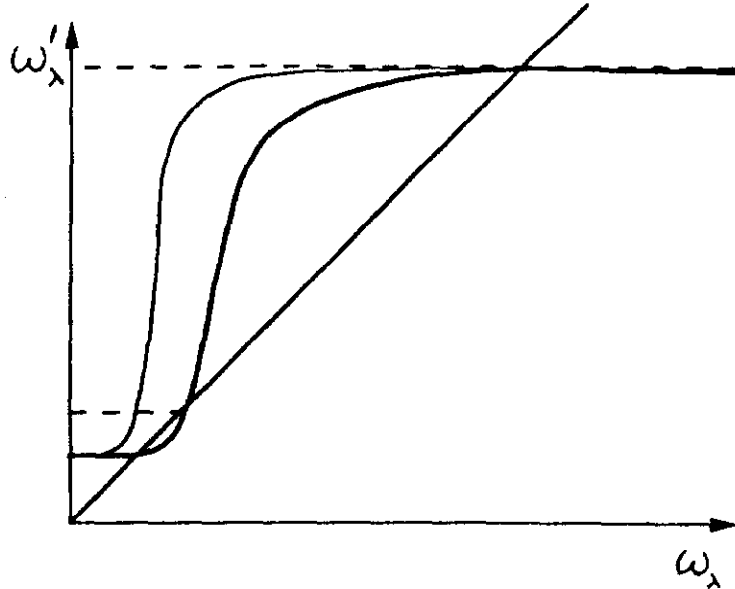


Fig.4 The eigenfrequency solutions of the dispersion relation (8). Thick line corresponds to the low eigennumber λ , when three intersections with the diagonal are present, and thin line shows the high- λ case with only one intersection.

The plateau of the r.h.s. graph at high frequency is determined by the condition $\mu \rightarrow 1$ for $\omega \rightarrow \infty$. It is clear that for low eigennumber λ and steep drop in $\mu(\omega)$ there are three eigenfrequency solutions, while for sufficiently high eigennumber λ only one, high-frequency solution is present. In the case of a more gradual roll-off of $\mu(\omega)$, there will be only one, low-frequency solution for the low eigennumber x_λ . The situation with the full complex-value dispersion relation is qualitatively similar, with low-frequency solution having small imaginary part $Im(\omega_\lambda)$, while the intermediate- and high-frequency solutions have a significant dissipation $Im(\omega_\lambda) \sim Re(\omega_\lambda)$. Indeed, as shown in Fig.5, taken from Ref./10/, the permeability μ becomes mostly imaginary for the frequencies significantly above the roll-off. The wakefield $W(s)$ of equation (7) consists of either one or several low wave-vector modes that correspond to the condition $\mu \approx \mu(\omega \rightarrow 0)$, and also consists of a given number of high wave-vector modes that correspond to

the condition $\mu \approx 1$. All high frequency wave-vectors $k = x_\lambda / \sqrt{\epsilon\mu - 1}$ are strongly dissipative $Re(k) \approx Im(k)$.

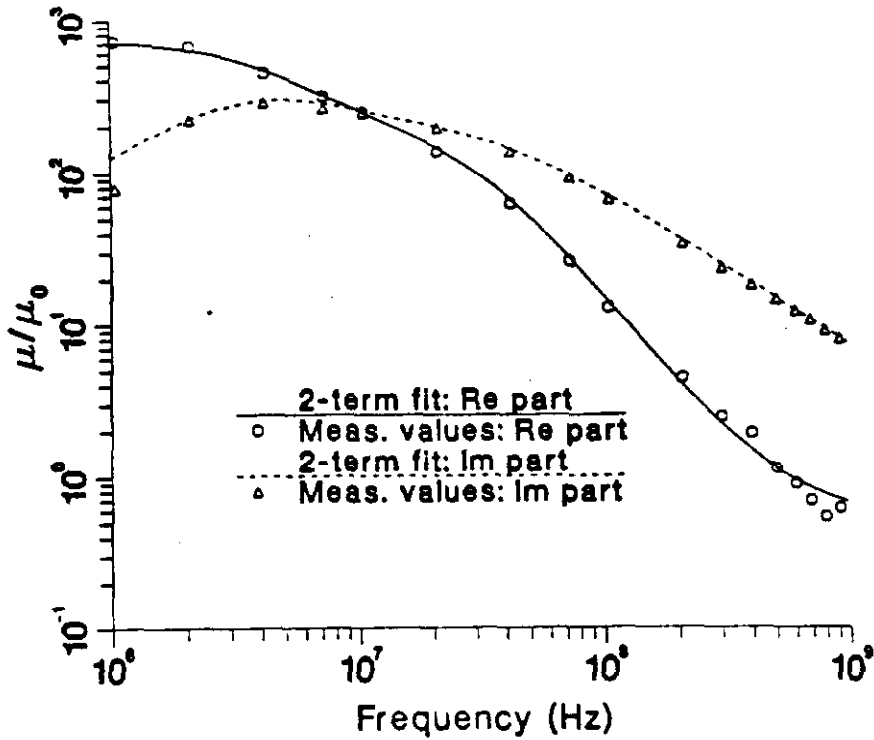


Fig.5 Real and imaginary parts of the permeability in a wide frequency range (Ref./9/).

The high wave-vector (high-frequency) modes are generally detrimental to the wakefield focusing, since they cause bunch lengthening when their wavelength is shorter than the bunch length /4/. Another important factor in choosing the optimal parameters of the waveguide is the unavoidability of fairly high frequencies, so that, e.g., the lowest-mode frequency $f_0 = 2.405c/2\pi a\sqrt{\epsilon\mu - 1}$ is 40 MHz for $a = 13\text{cm}$, $\epsilon = 10$ and $\mu = 70$. This lowest-mode frequency is approximately the roll-off frequency for these values of

permittivity and permeability. From these observations, more than one low-frequency mode is unlikely and therefore the thickness of the lining at the maximum is chosen which still yields only one mode (the “crossover regime”). The exact single-eigenmode condition is not available analytically, but can be estimated as the crossover from the thin lining to the thick lining case : $(1 - b/a) < 1/2\epsilon$. Since the eigenvalues x_λ depend on ϵ and a/b , but not on the permeability μ , we can use the information about the lowest eigenvalue $x_0 = \omega_0 a \sqrt{\epsilon\mu - 1}/c$ from the Ref./9/, shown in Fig.6.

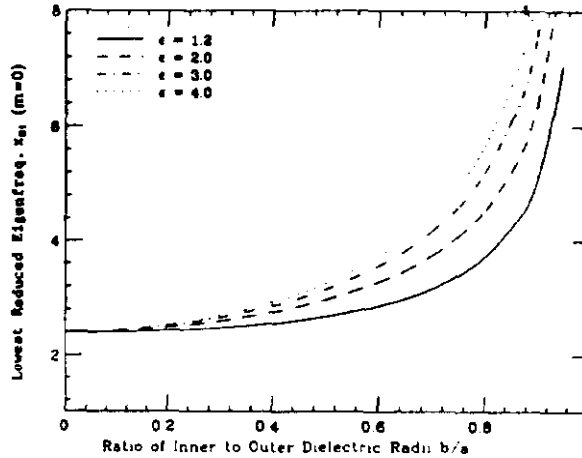


Fig.6 Lowest eigenvalue x_0 as a function of the inner/outer radii ratio a/b for different values of ϵ (Ref./9/).

It should be noticed that the reduction of the frequency of the lowest mode at the crossover from the thick lining case is the unavoidable consequence of eliminating the higher-order modes. That can be seen as well from the fact that the “effective length” (the distance at which the wakefield changes its sign) of the thick lining wakefield (6) is $\Delta s \approx b\sqrt{\mu/\epsilon}$, which is about equal to the lowest-mode wavelength at the crossover $\epsilon(1 - b/a) \approx 1$, $x_1 \approx 2\epsilon$.

A numerical simulation of the wakefield in a non-dispersive ferrite-lined cavity was performed using a recently developed code XWAKE /11/. The

shape of the cavity and the ferrite lining in the (radial-longitudinal) coordinates plane is shown in Fig.7.

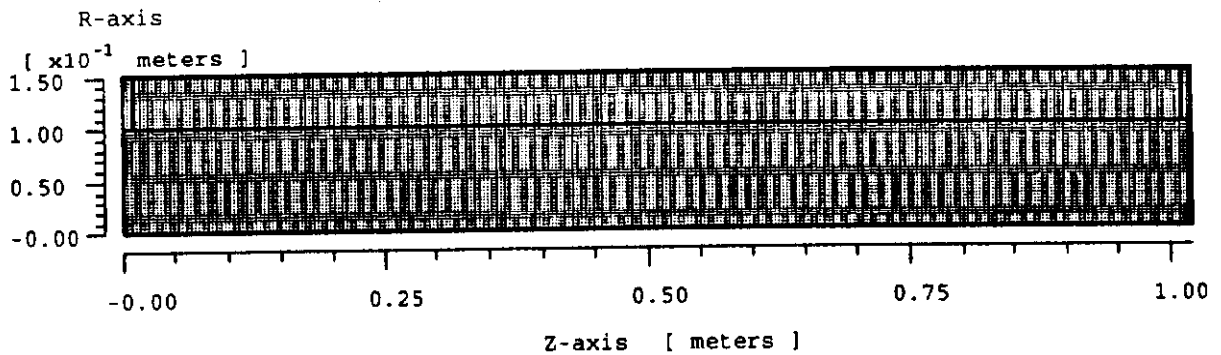


Fig.7 The ferrite-lined cavity shape for the XWAKE calculations of Figures 8 and 9.

The cavity structure is fully axial-symmetric and the pipe extends to infinity from both left and right ends of the structure, as provided for by suitable boundary conditions of the XWAKE code. The ferrite lining fills the space between the pipe radius b and the outer radius of the cavity a .

Two examples of the wakefields and impedances are shown in Figs.8 and

9. The thick lining case is shown in Fig.8.

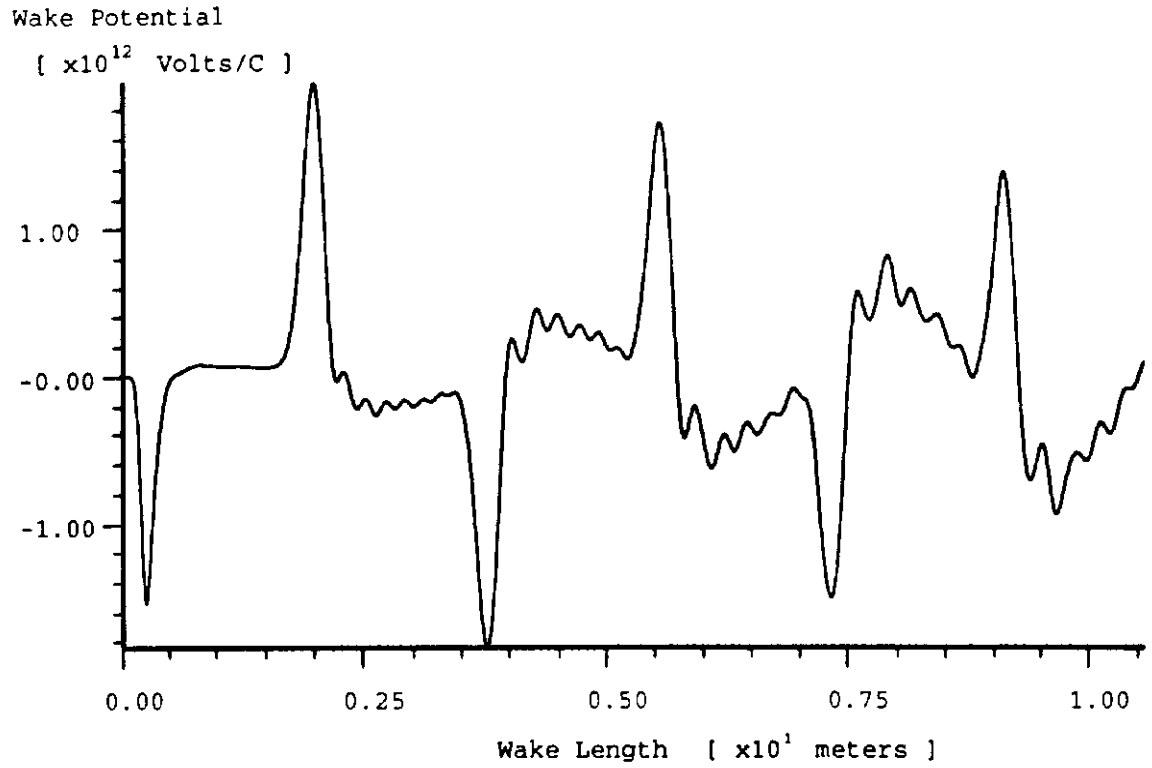


Fig.8a Wakefield $W(s)$ for the thick-lining cavity of the shape of Fig.7, with inner radius $b = 10$ cm, outer radius $a = 15.0$ cm, length $l = 100$ cm, and $\epsilon = 10$, $\mu = 25$.

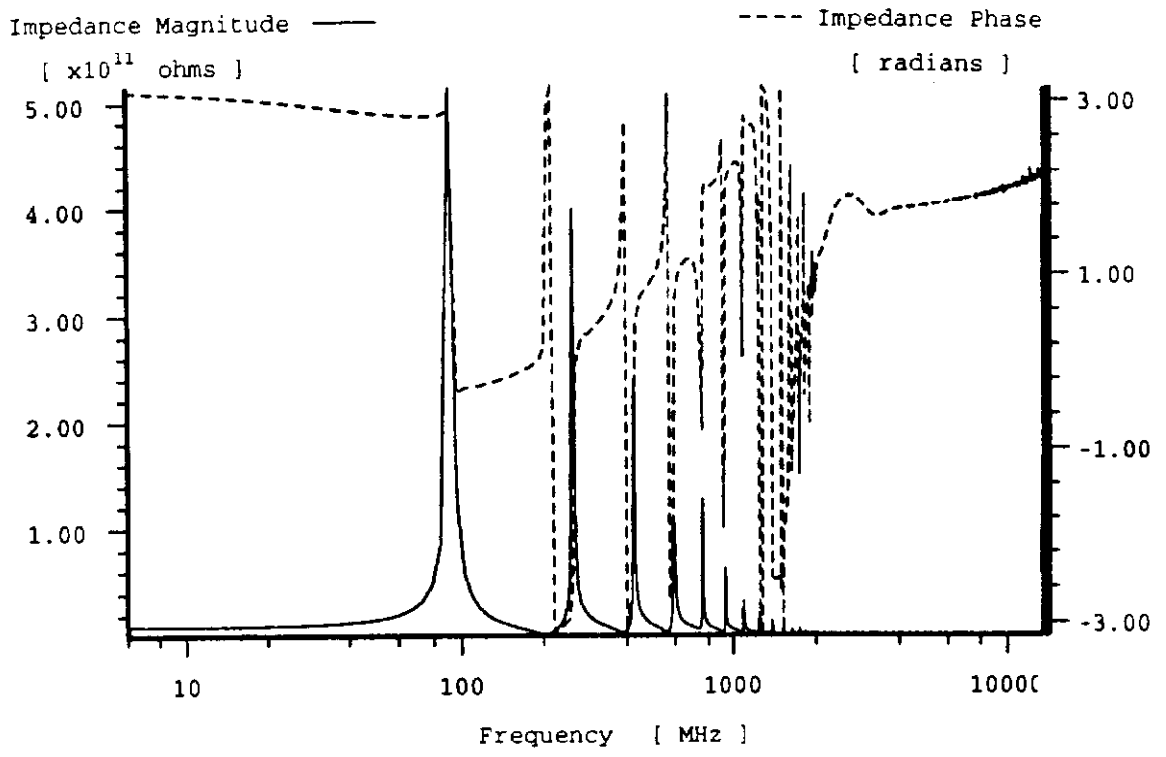


Fig.8b Impedance $Z(\omega)$ for the thick-lining case of Fig.8a.

The wakefield and impedance for the thickness $b/a = .90$ that is approximately the crossover for the ferrite parameters $\epsilon = 10, \mu = 25$, are shown in Figs 9a and b.

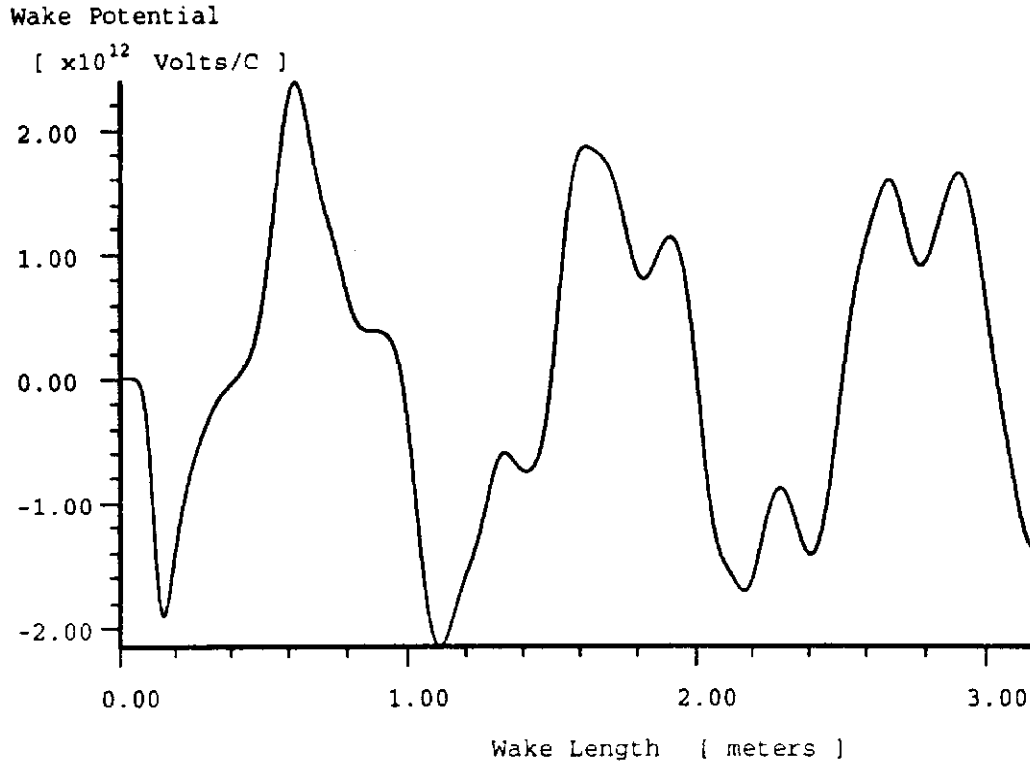


Fig.9a Wakefield $W(s)$ for the moderate-thickness lining with inner radius $b = 10$ cm, outer radius $a = 11.1$ cm, length $l = 100$ cm, and $\epsilon = 10, \mu = 25$.

The small higher-order modes that are seen in Figure 9 are assumed to be the consequence of the finite length of the structure. Based on a number of similar simulations for different ratios, the ratio $b/a = 0.90$ for $\epsilon = 10$ is chosen as the basis of the wakefield focusing device. The scaling with ϵ is $1 - b/a = 1/\epsilon$, while the frequency of the fundamental mode is $f_0 = c/6b\sqrt{\mu/\epsilon}$. The "effective length" of the wakefield is a quarter of the

wavelength $\Delta s = 1.5b\sqrt{\mu/\epsilon}$.

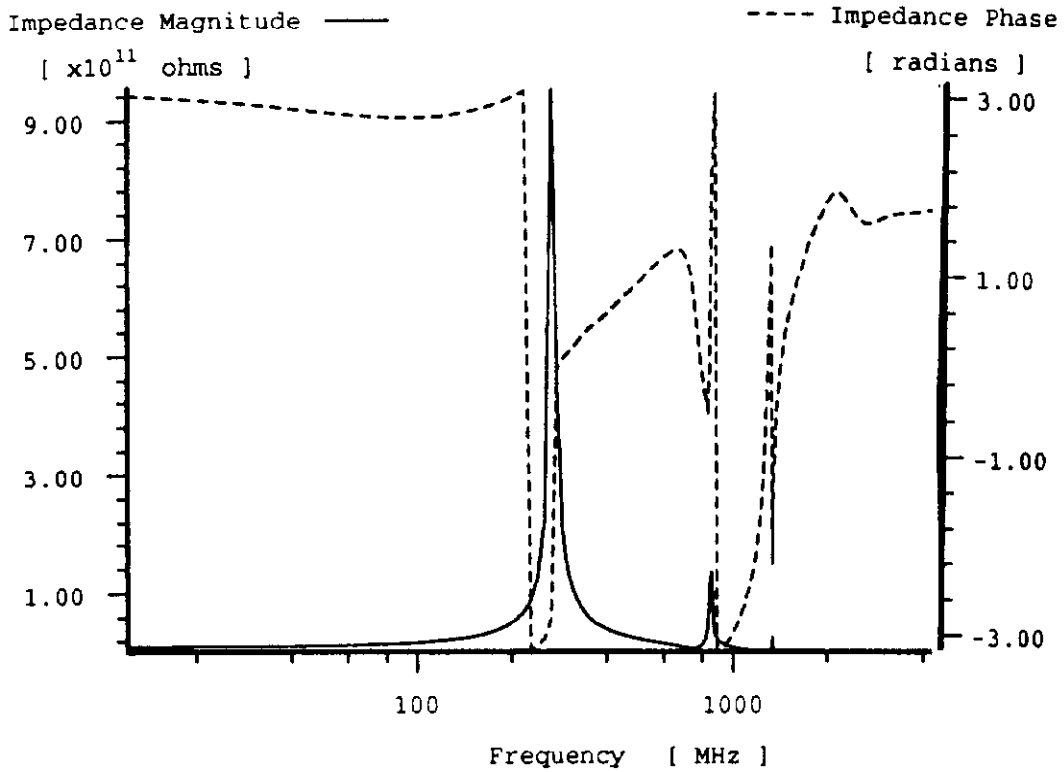


Fig.9b Impedance $Z(\omega)$ for the case of Fig.9a.

The results in Figure 9 allow to make some conclusions about the strength of the focusing voltage. The wakefield maximum W_{max} in Fig.9 is approximately $2.5 \cdot 10^{12}$ (V/mC), so the estimate for the decelerating field for an arbitrary a and ϵ is $E_{max}(V/m) = Q(C)2.5 \cdot 10^{10}/a^2(m^2)$. This voltage is independent of both the dielectric constant ϵ and permeability μ , similarly to the maximum wakefield in the thick-lining regime (6). For the bunches in Tevatron with $N_p \approx 10^{11}$ and the pipe radius $a = 10$ (cm) the decelerating gradient is $E_{max} \approx 40$ (kV/m).

A summary of the limitations of the scheme and design issues is presented in Section 4.

3 Collective and single-particle dynamics with wakefield focusing.

A separate computer code was written to simulate the beam dynamics in the presence of a given wakefield. The wakefield dependence on distance is the input function (one-dimensional array), and only a single bunch in the ring configuration was simulated.

3.1 Bunch compression simulation: broadband impedance.

Numerical simulation of bunch compression by the adiabatic increase of the wakefield was carried out by implementing the single-turn mappings for each particle. The RF focusing mapping is taken to be:

$$\bar{x} = x + p \quad (9)$$

$$\bar{p} = p - \frac{\omega_s^2}{\pi} \sin(\pi x) \quad (10)$$

where x, p are the longitudinal coordinate and momentum (relative to the equilibrium orbit), ω_s is the synchrotron frequency, and the units are such that the RF bucket length is $\lambda = 2$, while the revolution period $T_0 = 1$. This mapping is followed by the wakefield “kick” mapping:

$$\bar{\bar{x}} = \bar{x} \quad (11)$$

$$\bar{\bar{p}} = \bar{p} - \epsilon(t) \frac{\omega_s^2}{\pi} F(\bar{x}) \quad (12)$$

The normalized wakefield force, $0 < F(x) < 1$ is defined by the summation over all particles in the bunch that are in front of the point of consideration:

$$F(x) = \frac{1}{N} \sum_{x_j > x} F_0(x_j - x) \quad (13)$$

Here $F_0(x)$ is the point-charge wakefield that was taken to be $F_0 = 1$ for $x > 0$ and $F_0 = 0$ for $x < 0$ (a step-function wakefield, perfectly capacitive impedance). The wakefield intensity parameter ϵ is slowly increased from 0. to ϵ_{max} over the time period much longer than the synchrotron period $1/\omega_s$. The wakefield force depends only on the distribution of particles in the bunch *at this moment* but not at previous turns, which corresponds to the assumption of the wakefield completely decaying in one turn (broadband

impedance). Initial conditions for x and p were randomly seeded with the Gaussian distribution with the r.m.s. width 2σ for x and $2\omega_s\sigma$ for p .

Results of numerical simulation are presented in Figures 10-12. Fig.10 illustrates the bunch compression process for the parameter $\sigma = .1$ (which in our units is the same as the ratio of bunch length 2σ to RF wavelength λ). Parameter ϵ (as defined in expression (6)) is increased linearly in time from 0 to the maximum value ϵ_{max} . In Fig.10a, the center-of-mass displacement $a = \langle x \rangle$ of the bunch is shown as a function of time (measured in turns). In Fig.10b, the time dependence of the parameter σ which is the half of the r.m.s. bunch length.

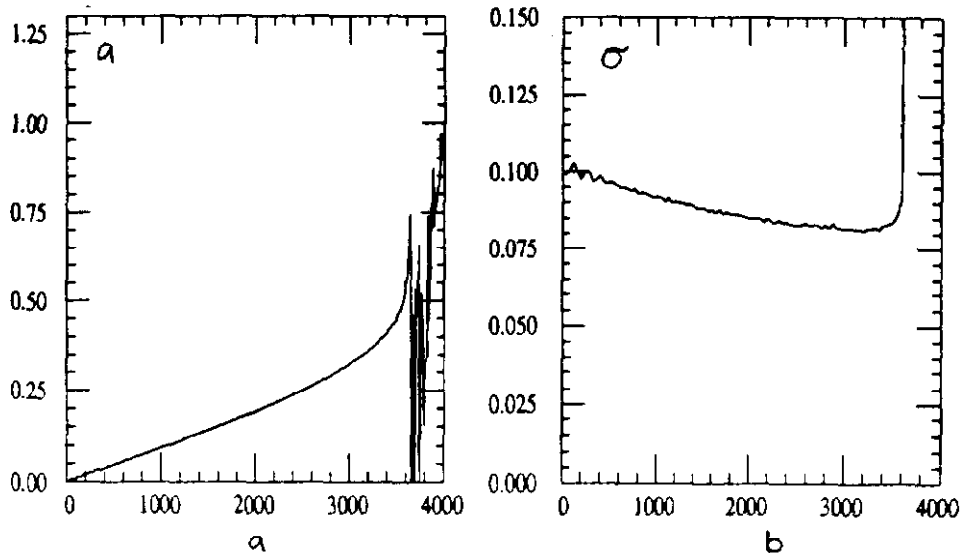


Fig.10a,b. Time dependence of (a) bunch displacement a , and (b) half bunch length σ for initial $\sigma_0 = .1$, $\omega_s = .1$ and $\epsilon_{max} = 2.1$. Time units are in turns.

Two important features found in the the graphs of Fig.10 below are a sudden increase in σ and oscillatory behaviour of the center of mass displacement, a , which occurs when a approaches $.5$. The reason for the observed behaviour of both σ and a is easily understood. When the energy loss of the beam per turn is larger than the RF voltage, the beam decelerates upon each turn in the ring and thus particles will be lost quickly. According to the

“beam loading” theorem (see, e.g. /12/), the energy loss of a short bunch due to a capacitive impedance is half of the decelerating voltage at short distances. Therefore, the threshold of deceleration approaches $W_{max}/V_{RF} = .5$ when σ is much less than 1. and the displacement a at the threshold approaches $a = .5$

To summarize the findings of the simulations, the adiabatic compression is working but the relative reduction of the bunch length for the realistic values of the ratio σ/λ_{RF} is quite small. Importantly, the compression factor G is independent of the synchrotron frequency ω_s , as long as the adiabaticity is preserved. On the other hand, from the arguments presented in the introduction the maximum achievable compression factor $G = \sigma_0/\sigma$ is increasing with the reduction of the initial size σ_0 (for constant λ). Two cases of smaller σ_0 are presented in Figs.11 and 12.

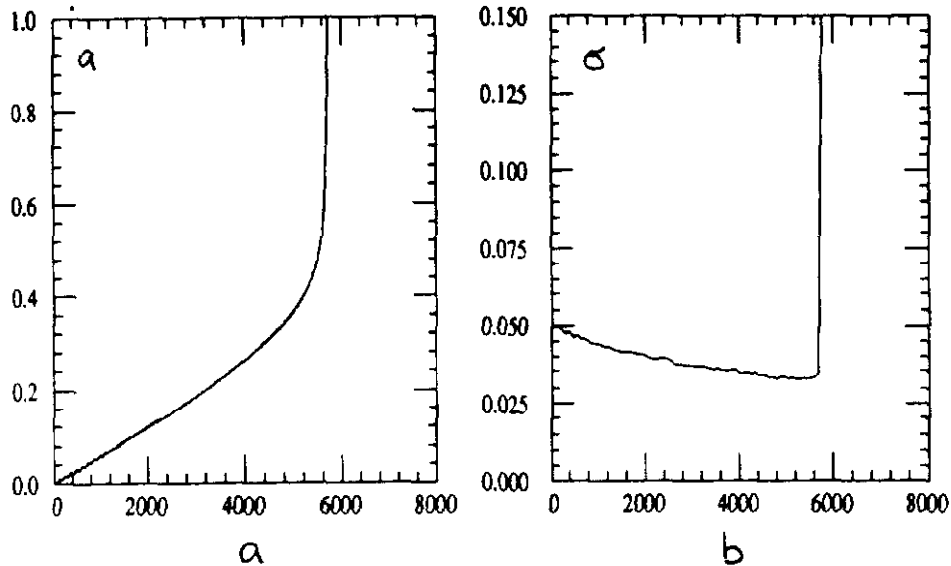


Fig.11a,b. Time dependence of (a) bunch displacement a , and (b) half bunch length σ for initial $\sigma_0 = .05$, $\omega_s = .1$, and $\epsilon_{max} = 2.1$. Time units are in turns.

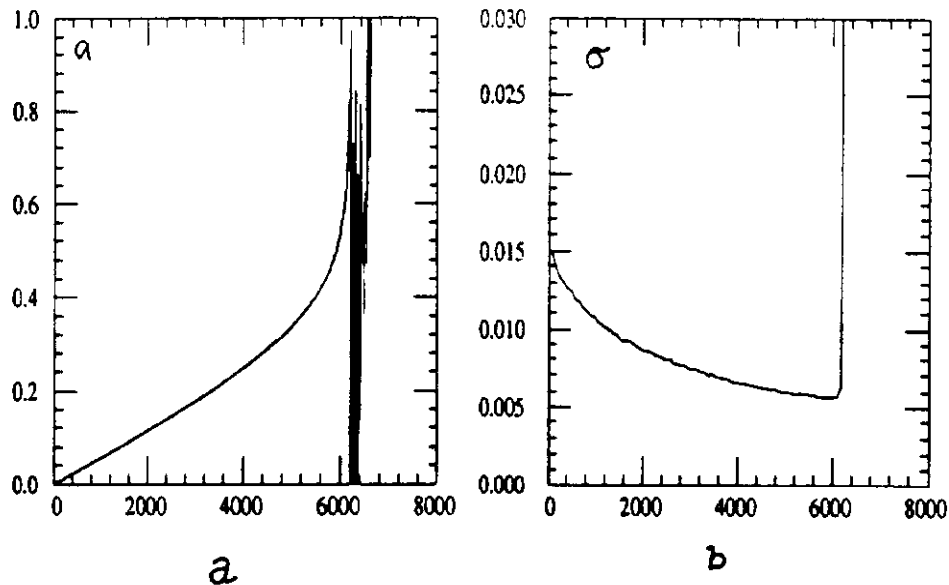


Fig.12a,b. Time dependence of (a) bunch displacement a , and (b) half bunch length σ for initial $\sigma_0 = .015$, $\omega_s = .1$ and $\epsilon_{max} = 2.1$. Time units are in turns.

As noted in the introduction, the compression factor G can be estimated from the phase space conservation to behave as $G \sim k^{1/3}$ for large distortion parameter, k . This estimate can be obtained from a two-particle (head-tail) approximation of the collective potential well. The large k regime can also be described as the situation in which most of the focusing is done by the wakefield rather than the RF field and bunch displacement a is much larger than σ . Because of the low power index in this scaling one would need a very small bunch to bucket length ratio, $\sigma/\lambda_{RF} \approx .025$, to be able to achieve the compression factor, $G = 2$. For the Tevatron, this ratio is much higher $\sigma/\lambda_{RF} \sim .1$, so no significant compression may be achieved in this manner.

3.2 Bunch compression simulation: narrowband impedance.

A rather discouraging conclusion of the previous section makes one search for a way of overcoming the major limitation imposed by the net deceleration of the bunch that comes along with the positive effect of focusing. The solution

is to “recycle” the energy of the wakefields and return it back to the beam. For the structures described in Section 2 this comes about quite naturally when the quality factor Q is high. Indeed, the parasitic energy loss U per revolution can be presented as (see, e.g. /12/):

$$U = 2\pi c^2 \omega_0 \sum_{p=-\infty}^{p=+\infty} |\bar{\rho}(p\omega)|^2 \operatorname{Re} Z(p\omega_0) \quad (14)$$

where $\bar{\rho}$ is the Fourier integral of the distribution function $\rho(x)$ and impedance $Z(\omega)$ is the Fourier integral of the wakefunction $W(ct)$. Assume now that the wakefield is determined by only one (fundamental) mode of the cavity:

$$W(s) = W_0 \left(\cos(ks) - \frac{1}{Q} \sin(ks) \right) \exp\left(-\frac{ks}{Q}\right) \quad (15)$$

where k is the wavevector of the mode $1/k \gg \sigma$ and Q is the quality factor. The corresponding impedance is:

$$Z(\omega) = \frac{2\pi W_0}{\omega_0 \left(1 + iQ \left(\frac{\omega}{\omega_r} - \frac{\omega_r}{\omega} \right) \right)} \quad (16)$$

where $\omega = c/s$, $\omega_r = ck$. The energy loss can be made arbitrarily small by achieving high Q if the resonant frequency ω_r is tuned not close to any of the revolution frequency multiples. The energy that is given to the wakefields on each turn is partially returned back. The total wakefield force F_m at m -th revolution has the contributions from the previous turns:

$$F_m(s) = \sum_{l=0}^{\infty} \int ds' \rho_{m-l}(s') W(lL_0 + s' - s) \quad (17)$$

where ρ_m is the distribution in the bunch at the m -th revolution and $L_0 = cT_0$ is the ring circumference. Using the condition of the wavelength $\lambda = 1/k$ that is much larger than the bunch length, one can present the above expression in a simpler form:

$$F_m(s) = \int ds' \rho_m(s') W(s' - s) + \sum_{l=1}^{\infty} W(lL_0 + a_m - s) \quad (18)$$

where a_m is the displacement of the bunch at the m -th revolution $a_m = \int ds s \rho_m(s)$. The first term in this expression is the “broadband contribution” that is the same as in the formula (13) in the previous section. The

last term comes from the previous turns. The relative magnitude of the two terms depends on the quality factor Q and the frequency ω_r . The second term will be large compared to the first when Q is high and the system is in resonance $\omega_r = h\omega_0$ (with h integer). This type of situation can be used for the longitudinal focusing by passive RF cavities (see, e.g. /13/). It does not provide however any significant advantages over the active focusing since the bunch sees the same quadratic potential well. In order to use the stronger effect of the wakefield (broadband) focusing, an off-resonance wakefield should be implemented. The magnitude of the second term then will be about the same as of the first, the parasitic loss will be small, and the amplitude of the fields in the cavity will be low. More details of this setup can be seen in the results of numerical simulation.

Two examples of the simulation result of the adiabatic bunch compression with the high- Q wakefields (narrowband impedance) are presented in Figs.13 and 14. The mappings and parameter definitions are the same as described in Section 2, except for the multi-turn component (second term in formula (18)). The parameters that specify the narrowband component are $\omega_r/\omega_0 = 514.5$ for Fig.13 and $\omega_r/\omega_0 = 514.3$ for Fig.14, together with $Q = 10290$ (which corresponds to the decay of the wakefield in 20 turns) and the main RF harmonic number $h = 1028$. Parameter ϵ (as defined in expression (12)) is raised linearly in time from 0 to the maximum value $\epsilon_{max} = 6.2$. Both of these cases have the wakefield wavelength that is much longer than the bunch length, so that the pure form of wakefield focusing

with a step-like wakefield is taking place.

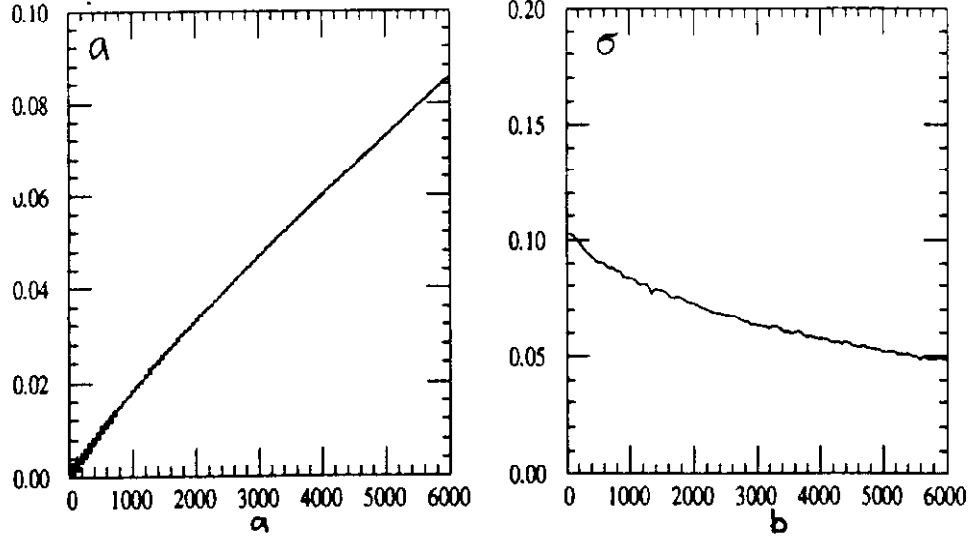


Fig.13a,b. Time dependence of (a) bunch displacement a , and (b) half bunch length σ for $\sigma_0 = .1$, $\omega_s = .1$, $\omega_r/\omega_0 = 514.5$, and $\epsilon_{max} = 6.2$. Time units are in turns.

In Figs.13a,b the bunch is focused to a significantly smaller size ($G \approx 2$), while the displacement of its center-of-mass is kept at a fairly low value. The latter is the indication of the low parasitic loss (small deceleration). This is also the reason why in this narrowband-impedance regime one can raise ϵ to so high a value, $\epsilon_{max} = 6.2$, without losing the stationary phase regime as in the broadband case. Some more insight into the nature of the process is provided by the graphs of Fig.13c, where the time series of the wakefield force coordinate dependence $F_m(s)$ are presented. Two curves in each graph refer to the full force $F_m(s)$ and its broadband component (first term in formula (18)). The broadband component is normalized so that it varies between zero in front of the bunch and 1 in its rear. For simplicity of calculation in simulation, when calculating this broadband component the step-function wake-function W , was used instead of the function (15). This is justified since the bunch is much shorter than the wavelength $\lambda = 2\pi/k$.

In the example of Figure 13 the short-range component of the wakefield is everywhere positive and thus produces a net deceleration. From the graphs of Fig.13c, the total force curve is shifted downward and the force is approximately zero at the location of the centre of the bunch. The latter in

these graphs is always in the centre of the “step” in the broadband component. Thus, the fields that ring for a long time return back the energy that is taken each turn from the beam.

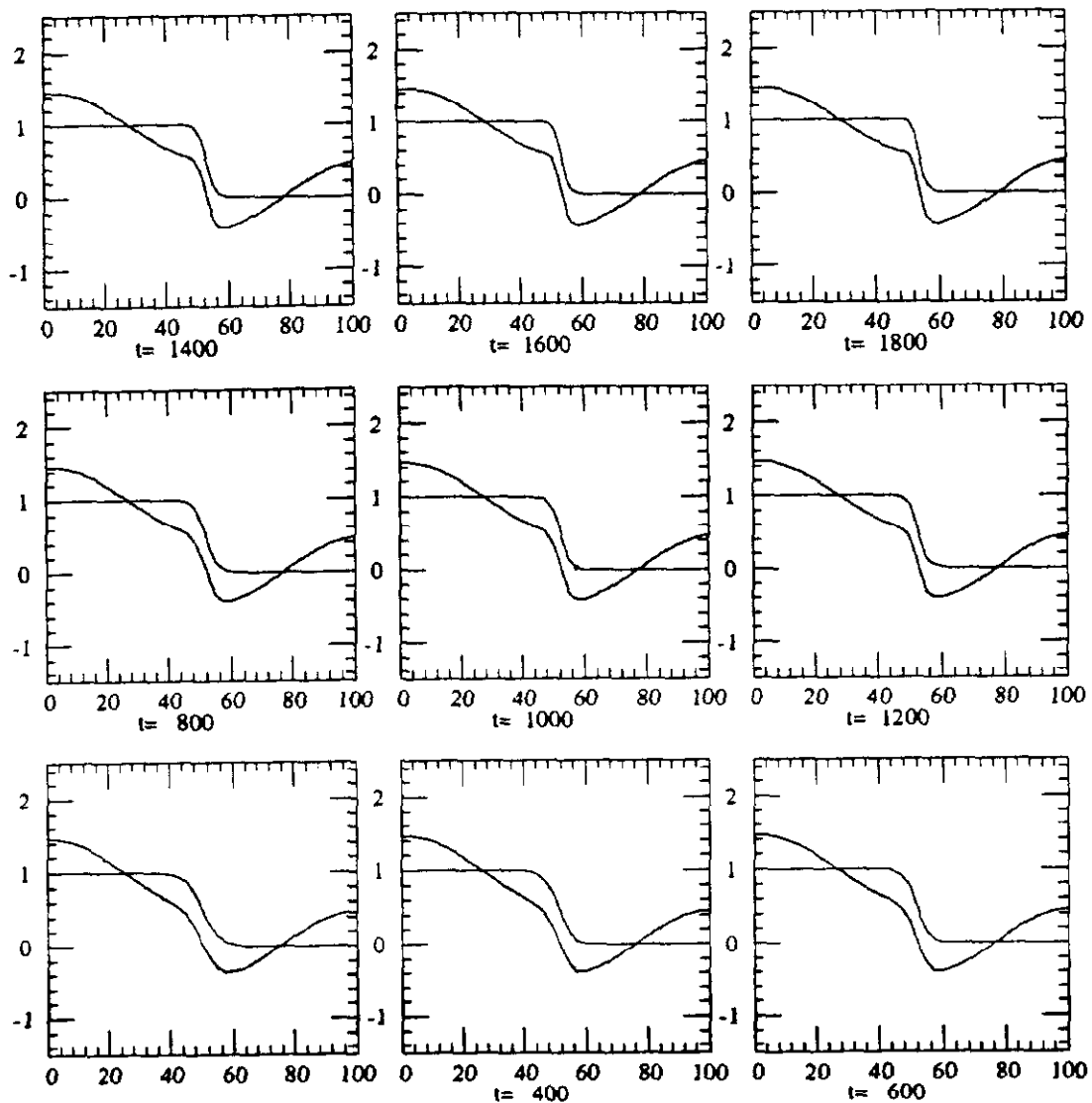


Fig.13c. Time series of the wakefield force dependence on coordinates for the case of Fig.13a,b. Horizontal scale is the period of the main RF $-1 < x < 1$. Time units are in turns.

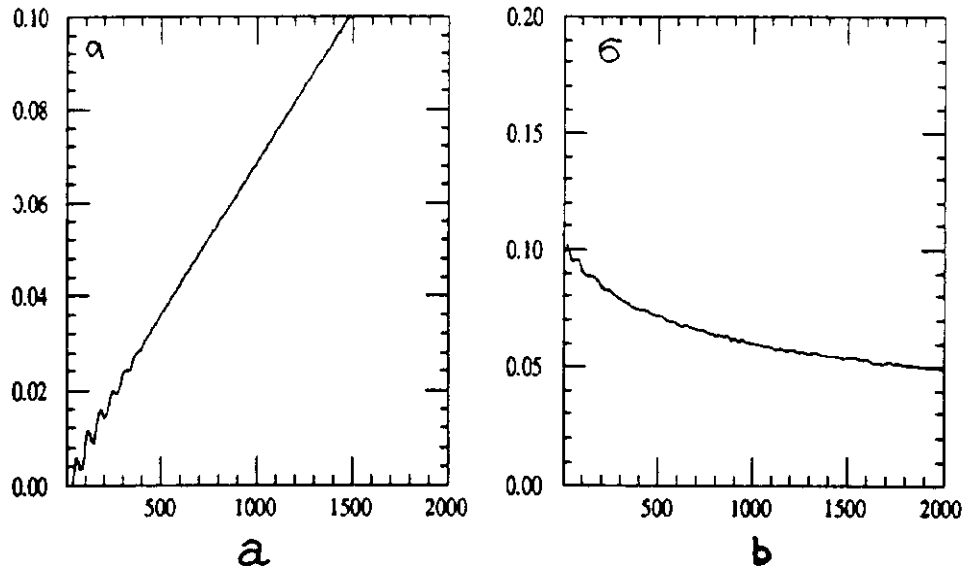


Fig.14a,b. Time dependence of (a) bunch displacement a , and (b) half bunch length σ for $\sigma_0 = .1$, $\omega_s = .1$, $\omega_r/\omega_0 = 514.3$ and $\epsilon_{mas} = 6.2$. Time units are in turns.

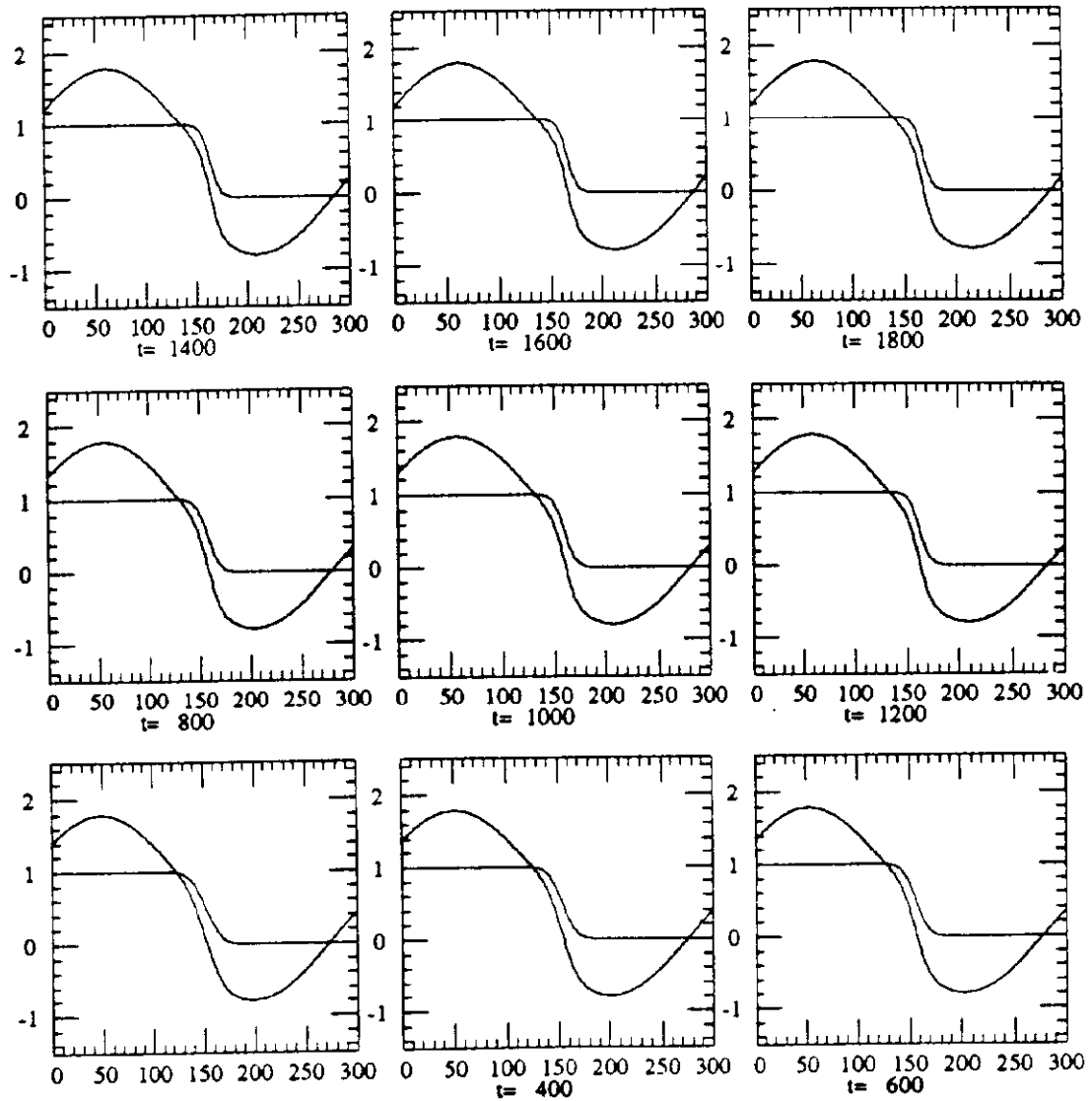


Fig.14c. Time series of the wakefield force dependence on coordinates for the case of Fig.14a,b. Horizontal scale is the period of the main RF $-1 < x < 1$. Time units are in turns.

The discussion of section 2.2 indicates that it would be very difficult to obtain the wakefield wavelength that is significantly longer than the bunch

length. An important question is what value of the wakefield wavelength to bunch length ratio is still acceptable. In Fig.15, the linear density profile evolution is shown for the adiabatic compression of the bunch, with the parameters $\omega_r/\omega_0 = 5140.6$, $Q = 5.14 \cdot 10^5$ (decay of the wakefield in 100 turns) and main RF harmonic number $h = 1028$. The wavelength of the wakefield λ in this case is twice larger than the (initial) bunch length $l = 2\sigma = .2$. The result of such shorter wavelength is the "spill" of the density in the adjacent potential minima of the total self-consistent potential well. A similar splitting of the bunch into sub-bunches was described in Ref./4/ for the electron machines with synchrotron damping. Most of the spill in Fig.15 is observed to be into the wakefield-induced "subbucket" which follows *after* the main sub-bunch (to the right of it). Some fairly small amount is spilled into the sub-bucket that is formed *in front* of the main sub-bunch. The total amount of spilled density in this case is estimated to be about 15% of the total. It was found that the smaller "spill" was achieved when the fundamental mode was tuned differently from the condition of "antiresonance" for the long wavelength, and hence a different frequency in the example of Fig.15. Shifting the frequency ω_r still higher causes, for so high quality factor, the onset of a (Robinson) instability, and the beam is observed to be lost.

The compression factor of the central sub-bunch, defined as the ratio of the maximum density in it to the maximum density in the initial bunch, is about 2.4, and is about the same as the compression factor for the long wavelength limit. If the wavelength-to-bunchlength ratio α is decreased still further, the amount of spilled density increases and the compression factors decrease. It is assumed that the trailing sub-bunch can be taken out of the machine in order not to interfere with the detector event identification. That can be achieved by manipulating the strength of the wakefield and the permeability μ (through the field biasing). The ratio $\alpha = 2$. appears thus to be about minimal acceptable and would result in a loss of about 15% of the beam.

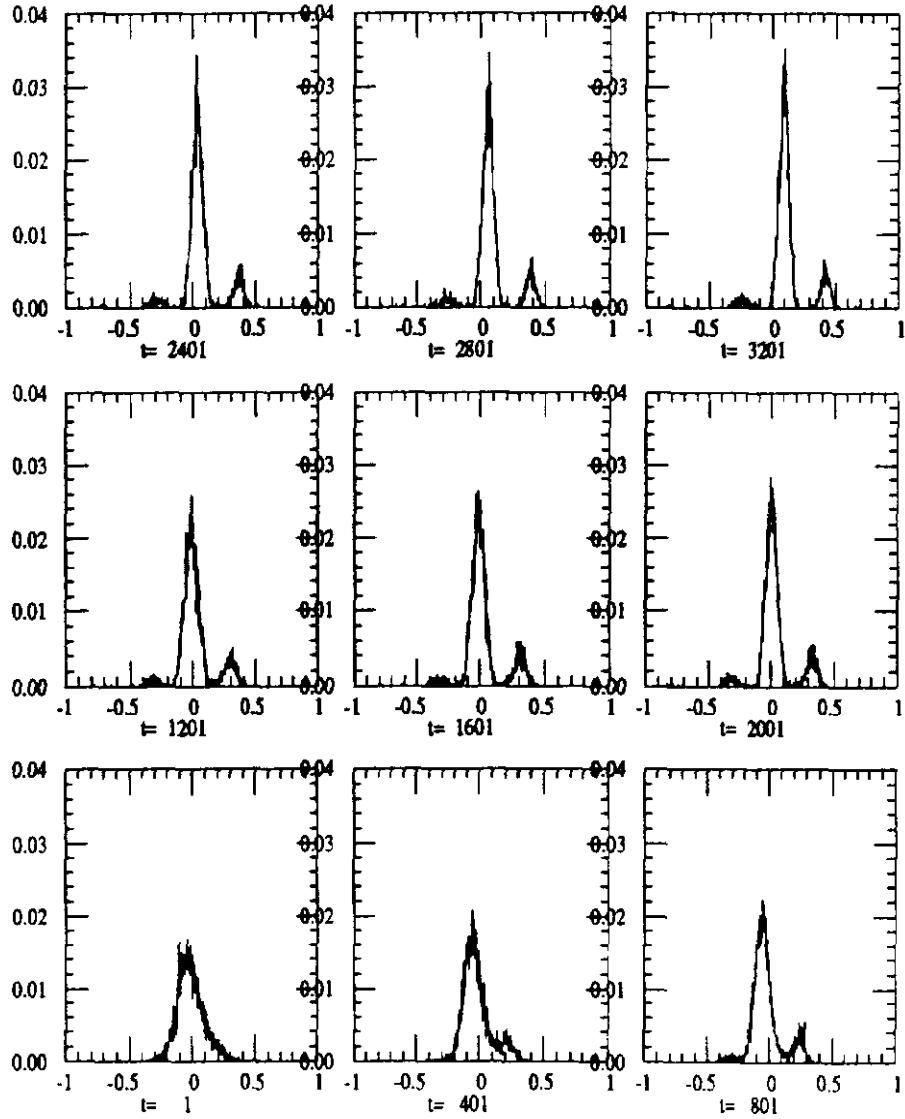


Fig.15. Time series of longitudinal density profiles. Horizontal scale corresponds to the period of the main RF $-1 < z < 1$. Time units are in turns.

Another important limitation that needs to be understood is related to the necessity of operating at as low a quality factor Q as possible, since the

choice of the permeability μ may be higher. From a number of simulations it was found that the system is significantly more tolerant of low Q 's for the smaller wavelengths than it is for the larger wavelengths. That property is to be expected since the power dissipation per turn decreases with the increase of the frequency of the wakefield. As an example, in Fig.16 the time series of the density profiles for a quite low $Q = 1.5 \cdot 10^4$ (wakefield decays in three turns) and $\omega_r/\omega_0 = 5140.8$, with the same initial bunch length as in Fig.15, are shown. The value of the frequency was optimized in order to reduce the "spill", and since the instability sets in much later at low Q 's, it is possible to operate much closer to the integer and reduce the spill to about 5%. No problems with the excessively large power dissipation appear yet, and the compression factor is about the same or even slightly higher. Further decrease of the quality factor was found to cause a deterioration of the compression factor, so we set the estimate for the minimum required Q as $Q_{min} = 3\omega_r/\omega_0 M$, where M is the number of bunches in the ring.

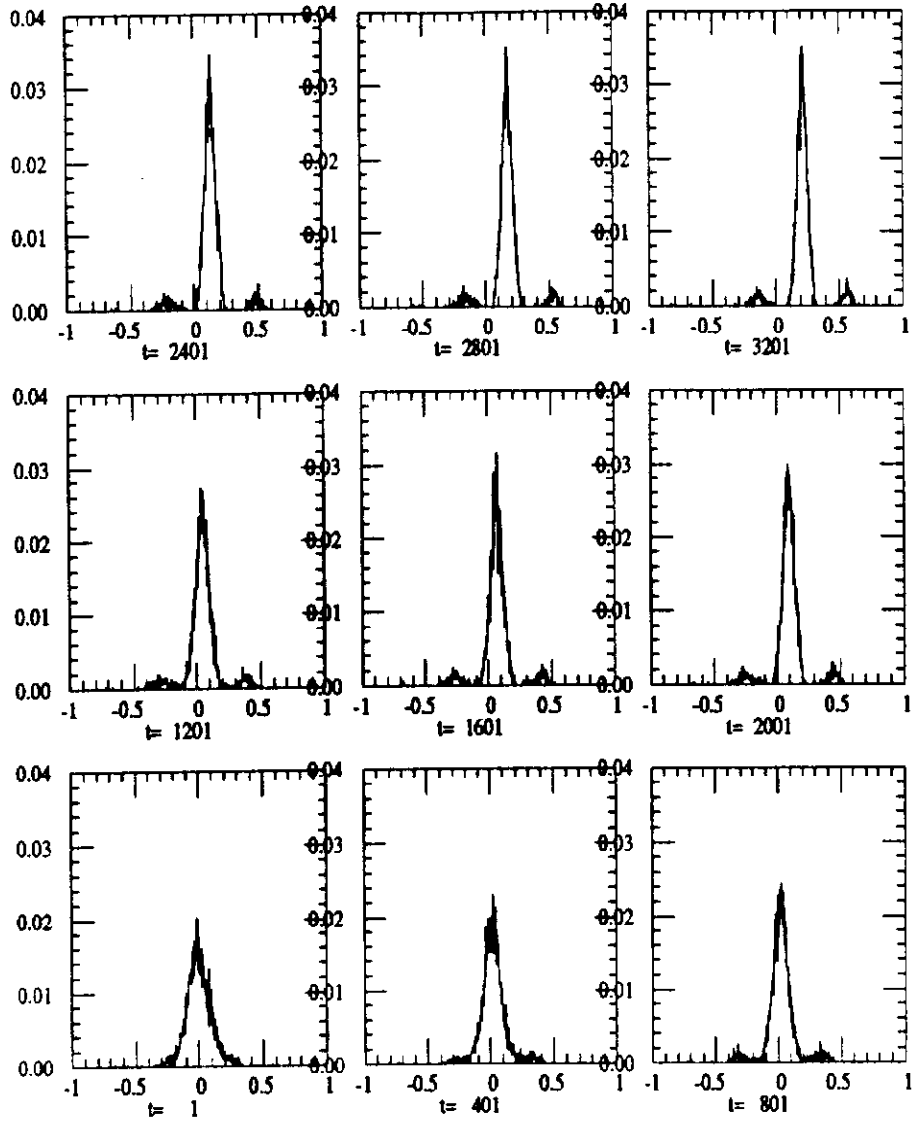


Fig.16. Time series of longitudinal density profiles for “low” quality factor $Q = 1.5 \cdot 10^4$ (wakefield decays in three turns). The horizontal scale corresponds to the period of the main RF, $-1 < x < 1$, and time units are in turns.

3.3 Coherent instabilities.

There is a host of stability problems that needs to be addressed in connection with the wakefield focusing scheme. Indeed, there is a huge longitudinal impedance together with a large transverse impedance, which is deliberately introduced in the ring. One may become rather skeptical about the prospects of providing stability when dealing with the longitudinal impedance that is several orders of magnitude larger than what is conventionally used. That challenge goes to the heart of the wakefield focusing concept: is it conceivable to tame the impedance and make it work for us rather than battle it?

The first stability result is provided by the numerical simulation of the preceding section: longitudinal, single-bunch dynamics is perfectly stable even with high- Q impedance (the wakefields that persist for many turns). The reason is twofold: first, the frequency of the narrowband impedance is tuned off-resonance, i.e. between the revolution harmonics, and second, the synchrotron tune spread becomes fairly large, $\delta\omega_s \sim \omega_s$, and grows together with the narrowband impedance. The longitudinal stability criterion that involves the ratio of the tune spread (Landau damping) to the impedance value is maintained at the same level at arbitrarily strong wakefield focusing.

The longitudinal stability with many bunches is not expected to present a problem due to the large longitudinal tune spread. Generally, if one chooses the frequency of the fundamental mode $l = 0$ from the Robinson stability criterion, the coupled-bunch modes $l \neq 0$ are always unstable in the absence of Landau damping. The estimate of stability criterion with the Landau damping is $\tau_{gr} \delta\omega_s < 1$, where the growth rate τ_{gr}^{-1} of a given multi-bunch mode l , without the Landau damping taken into account, is given by /12/:

$$\tau_{gr}^{-1} = \frac{\alpha N e^2}{2ET^2\omega_s} \sum_n [(Mn + l)\omega_0 + \omega_s] \text{Re } Z(Mn\omega_0 + l\omega_0 + \omega_s) \quad (19)$$

Here, α is the momentum compaction factor. For the detuned fundamental mode $f_{r0} \approx (k + .5)f_0$ and a relatively high quality factor $Q > 100$ the stability criterion for coupled-bunch modes is well satisfied.

The transverse stability of the system appears to be the most difficult one to provide for. Indeed, there is no significant Landau damping in the transverse planes while the transverse wakefield is growing together with the longitudinal wakefield. Since the longitudinal tune spread in the wakefield focusing regime is always large $\delta\omega_s/\omega_s \sim 1$, only the fast (relative to the synchrotron oscillations) transverse modes can go unstable. The stability criterion for the strong head-tail instability is $\eta = \frac{Ne^2W_sT_s}{8\omega_s m_0 \gamma} < 2/12/$, where

W_1 is the transverse dipole wakefield, T_s is the synchrotron period, and ω_β is the betatron frequency. The transverse lowest-mode dipole wakefield amplitude W_1 is related to the longitudinal lowest-mode wakefield amplitude W_l as $W_1 \sim W_l/a$ /9/, with the proportionality factor that depends on the ϵ and the thickness of the lining and is about .7 for $\epsilon > 3$ and our “crossover” thickness. The transverse wakefield is a sine-like function, so one has to include in the estimate the factor $\sin(2\pi\sigma/\lambda_{tr})$, where λ_{tr} is the wavelength of the transverse wakefield. That factor can not be much smaller than one, since at the crossover thickness the transverse wavelength is about the same as the longitudinal wavelength, while we can only hope to achieve the longitudinal wavelength that is twice larger than the bunch length. The stability criterion can be rewritten as:

$$\eta = \frac{.35T_s\Delta E}{a 2\pi R 8\omega_\beta m_0\gamma} < 2 \quad (20)$$

where ΔE is the total (longitudinal) energy loss by a particle in the bunch over the structure traversal. For the parameters of the Tevatron $f_\beta = 2.4\text{kHz}$, the twice larger synchrotron frequency $f_s = 60\text{Hz}$, and with $\Delta E = 4$ (MeV), $a = 10$ (cm), one obtains $\eta \approx 50$, which shows that one can not expect the beam to be stable transversely in a proton high-energy beam with a wakefield focusing. A feedback damping of the transverse instability would therefore be necessary. Since there will be only a single mode with a high $Q \geq 300$ to be damped, that should be possible to achieve. The wavelength of the transverse mode is about the longitudinal mode wavelength, since they are equal in the thin-lining case /9/.

4 Limitations summary and design issues.

Let us summarize the necessary conditions and limitations of the wakefield focusing with ferrite-lined waveguide.

1) The lining thickness should be chosen at the “crossover” $(a - b)/b \approx 1/\epsilon$ in order to eliminate the higher-order modes. The frequency of the fundamental mode then scales as $f_0 = \frac{c}{6b\sqrt{\mu/\epsilon}}$.

2) The inner radius of the ferrite channel b has to be large enough in order to obtain the “effective length” of the wakefield, which for the lining thickness so chosen scales as $\Delta s = c/4f_0 = 1.5b\sqrt{\mu/\epsilon}$, at least as long as the half-length of the bunch: $1.5b\sqrt{\mu/\epsilon} > .5l$.

3) The ferrite permeability roll-off frequency f_{r0} has to be larger than the frequency of the fundamental mode $f_{r0} > c/6b\sqrt{\mu/\epsilon}$, which presents a more restrictive condition on b than condition 2 if the bunch length is short $l < c/2f_{r0}$.

4) The quality factor of the ferrite Q at the fundamental frequency has to be large enough so that the energy of the wakefield of a bunch can be recovered by the following bunch: $QM f_{00}/f_0 > 3$, where M is the number of bunches, f_{00} is the revolution frequency and f_0 is the fundamental frequency.

5) Transverse impedance that accompanies the useful longitudinal focusing would make the head-tail modes unstable if no extra measures are taken. Broadband transverse feedback damping system is necessary, with the damping times of a few dozen turns.

6) The length of the waveguide that is required to reduce the bunch length by a factor of 2 is $L(m) = V_{RF}(V) b^2(cm^2) 1.7 \cdot 10^{-13} l / N \epsilon(C) \lambda_{RF}$ where V_{RF} is the RF voltage, λ_{RF} is the RF wavelength, and N is the number of particles per bunch.

It is clear, therefore, that the decision of the feasibility of wakefield focusing for proton rings hinges on the existence of a ferrite with high enough permeability μ and rolloff frequency f_{r0} . In order to minimize the radius b one has to choose the ferrite from one of the two conditions depending on whether the maximum μ_{max} of the function $f_{r0}(\mu)\sqrt{\mu/\epsilon}$ is smaller or larger than the root μ_r of the equation $f_{r0}(\mu) = c/2l$. In the former case, minimum b is achieved when the conditions 2 and 3 are equally restrictive, i.e. $f_{r0}(\mu_r) = c/2l$. The minimal radius then is $b_{min} = .33l/\sqrt{\mu_r/\epsilon}$. In the latter case, the minimum is achieved when $\mu = \mu_{max}$, yielding $b_{min} = c/6f_{r0}(\mu_{max})\sqrt{\mu_{max}/\epsilon}$. Using the family of ferrites from Fig.3 as an example, one can see that the quantity $f_{r0}(\mu)\sqrt{\mu}$ is a decreasing function of μ . Assuming the bunch length in the Tevatron (after Main Injector) to be $l = 30$ (cm), one obtains then the optimal ferrite from the condition $f_{r0}(\mu) = 500$ (MHz). The values $\mu = 7, \epsilon = 10$ for that frequency are achievable, yielding $b_{min} = 12cm$. Notice that the ferrites that operate at comparably high frequency with high enough Q do exist, such as a transversely biased aluminum-doped yttrium-iron-garnet (YIG) ferrite with $\mu \approx 7$ at 500 MHz, quoted in Ref./14/. The required length of the structure that would reduce the bunch length by the factor of 2 is obtained then from the estimate of item 6 to be $L \approx 73m$ for the $N_p = 10^{11}$ particles per bunch. If 36×36 bunches are to be used in the post-Main Injector Tevatron, the required quality factor is $Q \approx 900$. That does not appear to be a problem, since the ferrite-tuned cavity in the Ref./14/ (with the filling ratio of 12%)

had the quality factor $Q \approx 5000$.

In the case of the usage of shorter bunches with the same density while maintaining the same luminosity by proportionately increased number of bunches, the required length is smaller. Indeed, for $l = 15\text{cm}$ the optimal ferrite is defined by the condition $f_{ro} = 1\text{GHz}$. Assuming the value $\mu = 3, \epsilon = 10$ yields $b_{min} = 9\text{cm}$, which translates into $L = 41\text{m}$ for $N_p = 3.3 \cdot 10^{11}$ (same density N/l as in the previous case). It appears however that for so short bunches the dielectrics with $\epsilon \approx 3$ are preferable to the ferrites, since the ratio $\sqrt{\mu/\epsilon}$ and hence the wakefield wavelength stays about the same while the handling of dielectrics is substantially easier.

There was no mention so far of the means of a slow increase of the wakefield intensity. It appears at this point that the simplest way of doing that would be by using a retractable cylindrical screen on the inner surface of the ferrite. This may not be a convenient thing to do and more consideration needs to be given to this aspect of the scheme.

Only a single-bunch-in-the-ring dynamics of bunch compression by the wakefields was simulated so far. Several bunches of the same species (p or \bar{p}) will not change much the performance of the scheme and would in fact be helpful as it will proportionately reduce the Q requirement for the cavity. The energy from the wakefield in one bunch will be returned in that sense to the following bunch. The bunches of the different species can pass through the same structures without disrupting the energy balance if the structures are placed within an integer multiple of the structure wavelength from the interaction point. It is important to note that if the linear density of the \bar{p} bunches is the same as that of the p bunches, the different-species bunches will be compressed by the same factor even though the number of particles per bunch is widely different.

5 Conclusions.

The physics and technological issues of the wakefield focusing require more study, and the feasibility of the scheme may improve after more research is done. The major aspects of the problem that need clarification are: 1) Exact computation of the wakefields from the dispersive ferrites, 2) Possibility of equal focusing for unequal linear densities of p and \bar{p} bunches, 3) Energy balance and stability for several bunches of both p and \bar{p} . 4) Possibility of damping transverse instability with a feedback system. It is interesting to note that the usage of the ferromagnetic waveguide was proposed recently

for the purpose of the wakefield acceleration /15/.

One side effect of the wakefield focusing that may come out to be very useful is that the synchrotron frequency spread of the bunch increases drastically (since the wakefield potential well is inherently nonlinear). For the Tevatron bunch compressed by a factor of 2, the increase in the frequency spread can be estimated to be about 300 (times). This can be also extremely helpful for the bunched-beam momentum cooling (see Ref./16/).

6 Acknowledgements.

Many Fermilab people contributed to this work by sharing their expertise and giving useful advices. I am particularly thankful to Fady Harfoush for the help with TBCI and XWAKE calculations and to David Wildman for discussions of RF cavity properties. David Olivieri provided valuable help with improving the readability of the manuscript.

References.

1. P.Martin, Fermilab bunch length reduction, presentation at 4-th FNAL/SSCL Workshop on B Physics at Hadron Accelerators, November 17-17 1992, (unpublished).
2. Machine-Detector Interface Working Group Report, Proceedings of the Workshop on B Physics at Hadron Colliders, Snowmass, June 21-July 2 1993, Eds.P.McBride, C.S. Mishra.
3. A.Burov, Part.Accel.28 (1990) 47.
4. A.Burov, Bunch lengthening, self-focusing and splitting, Int.J.Mod.Phys.A (Proc.Suppl.) 2B (1993) 1148.
5. A.Burov, A.N.Novokhatski, Wake potentials of dielectric canal, ibid, p.537, The device for bunch self-focusing, INP Preprint 90-28.
6. K.Bane, Bunch Lengthening in the SLC Damping Rings, Accelerator Physics and Modelling Symposium, Ed.Z.Parsa,1993 (BNL-52379); K.Bane et al., Proc. of the 1st European Part.Accel.Conf., Rome,1988, p.878.
7. R.Baartman, Lectures at 1991 US Particle Accelerator School, unpublished.
8. T.Weiland, DESY 82-015, DESY-M-83-02 and NIM 213 (1983), NIM 215 (1983).
9. K.-Y.Ng Phys.Rev.D42 (1990) 1819.

10. J.F.DeFord, G.Kamin, G.D.Craig, L.Walling, Development and application of dispersive soft ferrite models for time-domain simulation, Accelerator Physics and Modelling Symposium, Ed.Z.Parsa,1993 (BNL-52379).
11. F.Harfoush, T.Jurgens, G.Saewert, XWAKE manual, to appear.
12. A.Chao, in *Physics of High En. Accel.*, Proc of the 2-nd Annual US Summer School on High En. Part. Accel., ed.M.Month, AIP Conf.Proc. No.105,1983.
13. A.Burov, A.Zholentz, Part. Accel. 28 (1990) 53.
14. L.Farley, G.Lawrence, J.Potter, Rapidly tuned buncher structure for the Los Alamos Proton Storage Ring, IEEE Trans. on Nuclear Science, V.NS-30, p.3511, 1983.
15. H.S.Uhm, Wakefield accelerator driven by a relativistic electron beam in a ferromagnetic waveguide, 1993 IEEE Particle Accelerator Conference Proc., v.4, p.2602, 1994.
16. J.Wei, Comparison between coasting and bunched beams on optimum stochastic cooling and signal suppression, 1991 IEEE particle Accelerator Conference Proc., p.1866; BNL-45514.